

# Statistical Signal Processing of Ultrasonic Signals in Norway Spruce Infected by Root and Butt Rot

Aferdita Aliu & Annika Tonteri  
October 25, 2011

Lund University, Faculty of Engineering

Maria Sandsten  
Supervisor at the Centre for Mathematical Sciences,  
The Division of Mathematical Statistics

Peter Ulriksen  
Supervisor at the Department of Measurement Technology and  
Industrial Electrical Engineering

Hans W Persson  
Supervisor at the Department of Measurement Technology and  
Industrial Electrical Engineering,

## Abstract

Root and butt rot in Norway spruce is costly for the forest industry and finding alternative non-invasive, efficient and cheap methods is thus of great interest. Detection of root and butt rot in Norway Spruce by analysis of an ultrasonic signal sent through standing trees could be a good alternative method. Data from Chirp-signals and sinus-waves, sent through both healthy and contaminated wood, has been used. The differences in the measured signals from the specimen, using both types of signals were analyzed with regard to their velocities and energy content. In addition the results from chirp measurements were used to analyze the differences in frequency content between healthy and contaminated wood.

## Acknowledgments

Since this master's thesis covers several academic fields we have had the great benefit of receiving support from several supervisors at Lund University, Faculty of Engineering.

We would therefore like to thank Peter Ulriksen, Engineering Geology, for devoting a lot of his time helping us with the experimental part of the thesis and Hans W Persson, Electrical Measurements, for his valuable input. We would also like to thank Maria Sandsten, Mathematical Statistics for answering the same questions over and over again.

# Contents

<b>1</b>	<b>Introduction.....</b>	<b>6</b>
1.1	Norway Spruce .....	6
1.2	Rot in trees and classification of decayed wood .....	6
1.3	Forestry in Sweden and financial aspects.....	8
1.4	Methods of detection today.....	8
1.4.1	Core sample .....	8
1.4.2	Acoustic testing.....	9
1.4.3	Electrical testing.....	9
<b>2</b>	<b>Purpose of thesis .....</b>	<b>10</b>
2.1	Using ultrasound.....	10
2.2	Other studies.....	11
<b>3</b>	<b>Theory .....</b>	<b>12</b>
3.1	Ultrasound .....	12
3.2	Wave propagation and behavior in trees .....	12
3.3	Chirp .....	13
<b>4</b>	<b>Method.....</b>	<b>14</b>
4.1	Samples and their preparation .....	14
4.2	Equipment and setup.....	15
4.3	Measurement methods.....	17
<b>5</b>	<b>Theory of spectral analysis .....</b>	<b>19</b>
5.1	Statistical measures.....	19
5.2	Spectral analysis.....	19
5.2.1	Linear filters and frequency function.....	20
5.2.2	Cross spectrum .....	20
5.3	The periodogram .....	21
<b>6</b>	<b>Linear regression models .....</b>	<b>22</b>
6.1	Simple regression .....	22
6.2	Multiple regression .....	22
6.3	Categorical variables .....	23
6.4	Residual analysis.....	24
<b>7</b>	<b>Results from data analysis – Sinus measurements.....</b>	<b>25</b>
7.1	The data .....	25
7.2	Energy analysis.....	25
7.3	Velocity analysis.....	28
<b>8</b>	<b>Results from data analysis – Chirp measurements.....</b>	<b>31</b>
8.1	The straight beam probe with exponential horn .....	31
8.1.1	The reference input signal .....	31
8.1.2	Peak to peak.....	32
8.1.3	Peak to rubber.....	33
8.2	Data alignment.....	34
8.3	Frequency analysis.....	35
8.3.1	Coherence spectrum analysis in two intervals.....	39
8.3.2	Coherence spectrum analysis in three intervals.....	41
8.4	Energy analysis.....	42
8.5	Velocity analysis.....	43
<b>9</b>	<b>Discussion/Analysis.....</b>	<b>45</b>
9.1	Results .....	45
9.2	Future work .....	45
9.3	Conclusions .....	46

<b>10</b>	<b>Appendix A</b> .....	<b>47</b>
10.1	Tables from one frequency measurements – Series 1 .....	47
10.1.1	<i>Energy analysis</i> .....	47
10.1.2	<i>Velocity analysis</i> .....	48
10.2	Tables from chirp measurements analysis – Series 3.....	49
10.2.1	<i>Frequency analysis</i> .....	49
10.2.2	<i>Energy in interval <math>I_2</math> of coherence spectrum (Section 8.3.2)</i> .....	50
10.2.3	<i>Energy analysis</i> .....	50
10.2.4	<i>Velocity analysis</i> .....	51
<b>11</b>	<b>Bibliography</b> .....	<b>53</b>

# 1 Introduction

Finding a non-invasive effective low-cost method for detecting root and butt rot in standing trees is for several reasons of great interest. Root and butt rot have a severe biological and economical impact on forestry in Sweden.

Norway Spruce, *Picea abies*, an economically important tree species, commonly grown in Sweden, is used in this study. The quality of the wood is crucial since there is a greater economic gain when the wood is sold as timber; wood used as timber is required to be of good quality. The financial loss due to rot in trees is noteworthy<sup>1</sup>.

Methods used today are mainly invasive and can harm the tree and affect its growth in a negative manner. Alternative methods would have significant effects to the forest industry in Sweden.

Ultrasound is a fairly cheap non-invasive method and could prove to be an excellent method for detection of any decay. It is also easy to handle and would give a quick result. The question is if it will give an absolute result for initial stages of decay, a level of precision needed if the method is to be considered a good alternative.

## 1.1 Norway Spruce

The measurements done to determine the suitability of ultrasound are all done on wood from Norway Spruce, *Picea abies*, a native European species. It is of great importance to European forestry as well as for the continents economy as a whole<sup>2</sup>. Within forestry Norway Spruce is used mainly as timber and for production of paper.

A Norway Spruce will be 30-40 m high when fully grown and it will normally live 250-350 years. The root system is shallow, thus sensitive to too cold wind, weather and draught<sup>3</sup>. Norway Spruce can be infected with root and butt rot, a fungus common in Swedish forests.

## 1.2 Rot in trees and classification of decayed wood

Root and butt rot are common types of fungus found in Norway Spruce. The rot is due to pathogenic fungus, which only occurs, in living trees. Annosus root rot<sup>4</sup>, caused by a polypore fungus is one of the main concerns within Swedish forestry today. It causes 75% of all rot in trees within Sweden<sup>5</sup>. This percentage has grown since forestry has undergone changes and forest work is being done around the year. The polypore fungus decomposes the woods cellulose from the bottom and up creating a cone consisting of porous matter. As the fungus decomposes the cellulose and lignin in the wood, it becomes soft<sup>6</sup>, thus altering its physical properties. The fungus can be found in both the roots as well as the stem of the

---

1 Matts Lindbladh, *Granens biologi*, Institutionen för Sydsvensk Skogsvetenskap  
<http://www-gran.slu.se/Webbok/PDFdokument/Biologi.pdf> p.6

2 <http://www.fs.fed.us/database/feis/plants/tree/picabi/all.html> 110623 15:00

3 <http://www-gran.slu.se/Webbok/PDFdokument/Biologi.pdf> p.2

4 sv. rotticka

5 <http://www-gran.slu.se/Webbok/PDFdokument/Biologi.pdf> p.14

6 <http://www.skogforsk.se/sv/KunskapDirekt/Gallra/Rota-och-andra-svampskador-/>, 110621 15:16 p.5

tree. It can be contaminated through the roots and cicatrices<sup>7</sup> the stock of the tree. In spruce the rot can often be found rather high up in the tree, compared to other species. Rot in the tree often affects the growth of the tree, generating further costs due to loss of potential timber. The strength of the wood alters in a negative manner with rot and trees with decay are often subject to weather related cicatrices. The wood also becomes discolored in such a way that it cannot be sold as building timber due to cosmetic demands on such material. In spruce, chopping off the contaminated section of the tree can salvage some of the wood. However this handling of the wood is time-consuming and costly.

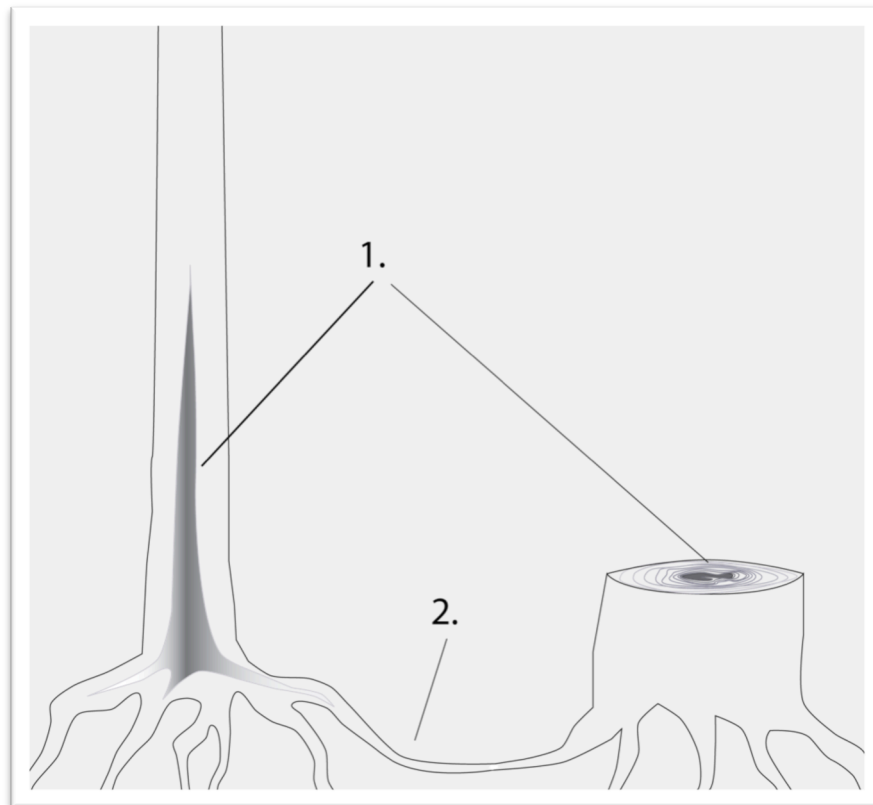


**Figure 1.1** 1.Examples of root and butt rot. Notice that the rot in the tree stem is cone shaped. Although the tree on the right has been felled, it may still cause problems, contaminating its surroundings.  
2. Shows how the roots are connected between the trees. In this way the trees can be contaminated by the root system.

Furthermore one problem is that root rot is spread by the root system. In a forest, finding one tree contaminated by rot, it is likely that several others will be so as well.

The economical value of a forest would be much easier to estimate if the forest owner would be able to evaluate which trees are contaminated and which are not. Decisions to disforest would also be easier to make and the rot could be more easily controlled and stopped from spreading and trees in danger of falling could be felled.

The degree of decay in a tree may affect the mechanical properties within the tree; the sound wave may no longer behave in the predicted way. One of the most important demands on a method for detection of rot in standing trees is to detect decay in the initial stages.

<sup>7</sup> sv. Skada, ärr inom botanik

### 1.3 Forestry in Sweden and financial aspects

Forests provide a renewable source of raw material, a versatile material that can be used in a number of products. Sweden has an area of 450 295 square kilometers, of which roughly a half is covered with forest. Pine and spruce being most common species, as much as 41% of Swedish forests consist of spruce.

Forestry has been, and will be, an important part of Sweden's livelihood. Even today forestry or forestry related industry, such as paper industry, provide 200,000<sup>8</sup> job opportunities.

The forest industry has a huge impact on Sweden's economy being one of the country's main resources. It accounts annually for 10-12% of the country's economy within its industry<sup>9</sup>. The forest industry contributes significantly to Sweden's trade balance, 70-80% of the products such as timber and paper being exported.

The loss of good wood to rot related damages results in a financial loss due to reduction in value is approximated to 500-1000 Msek annually<sup>10</sup>. Because of this the need for an improved method is of great importance and interest.

### 1.4 Methods of detection today

Several methods for detecting rot are today used within forestry. Most of them do not satisfy the demands on a method being time efficient, economical, exact and easy to use.

Only trees contaminated for a long time can visually be detected with rot. In these cases the probability of the surrounding trees being contaminated is significant. The information from this visual detection is irrelevant when estimating an area containing contaminated trees since it is mainly of interest to find the trees on the boundaries.

Some non-invasive methods have been investigated, such as X-ray, computer tomography and magnetic resonance, but have proven to be too costly and complex. The ultimate method would be non-invasive, low cost and time efficient.

#### 1.4.1 Core sample

A common, but time consuming, invasive method used to detect rot is by drilling a hole in the tree stem and inspecting the core sample. This is however destructive and may have a negative effect on the future growth of the tree. There is also a risk of not finding any rot in a tree, although it may very well be contaminated by rot, by drilling in the wrong place. In cases when the tree is found to be healthy the hole left in the stem left by the core sample also makes the tree more vulnerable for contamination in the future. This method cannot be used in an effective way in forestry since it is very time consuming, imprecise and invasive. It may damage the tree, counteracting any benefits in the long run.

---

<sup>8</sup>*The Swedish Forest Industries, Facts and Figures 2010*, Brommatryck & Brolins, May 2011. p.5

<sup>9</sup>*The Swedish Forest Industries, Facts and Figures 2010*, Brommatryck & Brolins, May 2011. p.4

<sup>10</sup> <http://www-gran.slu.se/Webbok/PDFdokument/Biologi.pdf> p.6

### 1.4.2 Acoustic testing

Using the fact that the fungus alters the trees physical properties, one of the ways of detecting rot in trees is by using the acoustics of the tree. By knocking on the wood a well-trained ear can hear the difference in the resonance between a healthy tree and a tree made hollow by the fungus. This method also demands the tree being largely affected by rot before any differentiation can be made. The method is also very imprecise and can only be evaluated subjectively.

There are however some examples of more sophisticated methods where acoustics are being used, both *Picus*® and *ARBOTOM*® use acoustics. They have however proven to be too complex to be able to be used in the field<sup>11</sup>.

### 1.4.3 Electrical testing

A new way of testing has been developed using the fact that the resistance and thus the conductivity in the tree alter depending on the degree of rot. A healthy tree has a stronger resistance than a contaminated one. The detection measurement with a *Rotfinder* takes only 10-15 seconds and works well in the field as long as the tree is not frozen and has a diameter of 10-80 cm<sup>12</sup>. Bengt Bengtsson at Lund University, Faculty of Engineering and the Swedish Forest Institute “Skogforsk” have developed the *Rotfinder*. This method seems to be a rather feasible method.

---

<sup>11</sup> <http://www-gran.slu.se/Webbok/PDFdokument/Rötbok%20fullständig%201%2020060626.pdf> 110920 21:02

<sup>12</sup> [http://www.websitefolder.net/rotfinder/Historien\\_om\\_Rotfinder.asp](http://www.websitefolder.net/rotfinder/Historien_om_Rotfinder.asp) 110920 21:12

## 2 Purpose of thesis

Although there today are several methods available for detecting rot, none of them satisfy all the demands on an ultimate method.

An alternative method, using ultrasound, could be a possible way to examine the extent of rot in a tree. Analysis of the alteration of signal sent through a log and comparison between the resulting signals from a healthy tree and an infected one may be a good method.

As the measurement of root and butt rot is assumed to take place when the tree is standing in the forest, the method needs to be quick and efficient. Large apparatuses have to be ruled out and there should not be any demands on the user being educated in detecting decay, more than in the use of the device.

One of the purposes when wanting to find rot in trees is to know which part of the forest to disforest. In this process it is important to find the contaminated trees and estimate the extent of the damage and the area the fungus has spread to. Therefore the equipment used to send and catch the signal needs to be quick to use and the equipment easy to install since there is a need to analyze several trees in order to be able to make a good estimation.

The device needs to be cheap as well as insensitive. It will be used in demanding environments by several different users adding to the need for it to be robust but cheap to replace in case of an accident.

As in all measurements it is beneficial for the measurements to be precise. Although there is no demand on always knowing the extent of the damage caused by the fungus, whether or not the tree is infected is crucial information and needs to be definite. When determining the boundaries of the infected specimen, the apparatus needs to be precise enough to find indication of decay even in its initial stages.

Invasive methods may affect the growth of the tree as well as its resistance to future contamination. A non-invasive method gives results without damaging the tree, avoiding future financial losses.

### 2.1 Using ultrasound

Using sound waves and ultrasound is a simple method compared to some of the advanced imaging methods that have been investigated, such as computer tomography (CT) and magnetic resonance (MR).

In short ultrasonic waves can be sent through a standing tree using two exponential horns. One sends the signal and the other receives it on the opposite side. The travel time of the wave through the tree is determined by the structure of the tree stem<sup>13</sup>. Presence of rot alters the wave and the received signal can be analyzed in different ways to try to determine if the tree is infected or not. Ultrasound seems to be a good alternative method for detection of rot in standing trees satisfying the requirements stated above.

The method of ultrasonic waves is not as expensive as other newly developed methods. The

---

<sup>13</sup> X. Wang, F. Divos, C. Pilon, B. Brashaw, R. Ross & R. Pellerin, *Assessment of Decay in Standing Timber Using Stress Wave Timing Nondestructive Evaluation Tools*, U.S. Department of Agriculture, Forest Service, Forest Products Laboratory, Madison, WI. 2004. p 1

exponential horn used is fairly robust and cheap compared to other alternative devices. The price of a device would be reasonable.

When using ultrasound, only two small areas of bark need to be removed to be able to reach the surface of the stem, minimizing any lasting impact on the tree. The tree is left without major damage, removing the bark does not damage it. Placing the exponential horns and sending the signal does not require any specific knowledge, as long as the algorithms used for detection are already applied. The measurements can furthermore be done on standing trees, this being an important fact when minimizing damages caused by rot.

## 2.2 Other studies

Other studies using ultrasound as a method of detection of decay in infected trees have been conducted. These studies have however often been done on timber or logs, not on standing trees. These results are meant to be used to find decay in e.g. built structures.

Other studies show that there occurs an attenuation of the signals when the wave passes through a subject with decay<sup>14</sup>. However the problem with using this method is that it only gives definite results when the decay has developed further on than in the initial stages.

When an ultrasound wave is sent through the tree the wave chooses to make its wave around the area of decay. This extends the time of flight of the signal (Figure 2.). We also know from the biological facts that the rot forms a cone from the bottom and up (Figure 1.) This affects the results of an experiment.

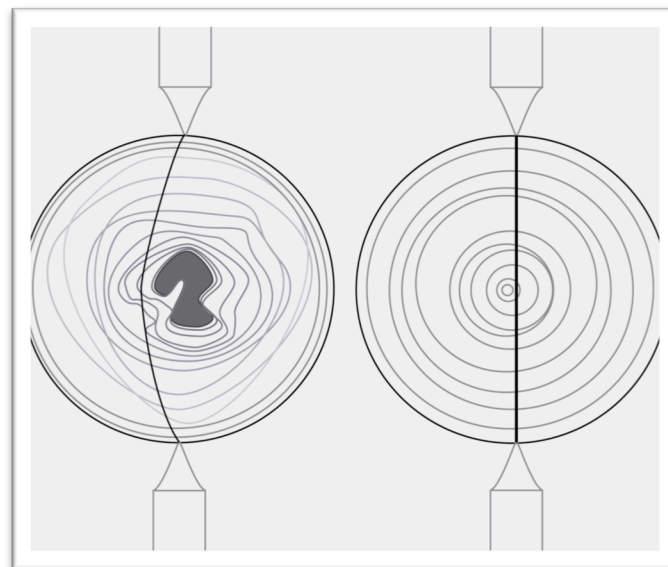


**Figure 2.1** *Illustration of how the waves pass through a tree with and without rot.*

---

<sup>14</sup> V. Bucur, *Acoustics of Wood*, Springer-Verlag Berlin Heidelberg New York, 2006

## 3 Theory

### 3.1 Ultrasound

The human ear is limited to hear sound waves up to a certain limit. This upper limit differs between individuals but is often approximated to 20 kHz. Sound waves with a greater frequency are referred to as ultrasound. The basic principles of waves govern ultrasound.

Use of ultrasound can be found in nature, e.g. bats use ultrasound to navigate. Bats use echolocation by sending out a signal that then bounces off surrounding surfaces, echoing back to the bat. This way the bat is able to determine the distances and contours of surrounding objects, creating a “map” without the use of visual aid.

One of the most commonly known applications of ultrasound is medical examination with ultrasonography producing a picture of a fetus in the womb. In a similar way to the bats the ultrasound wave reaches thresholds from one matter into another creating a reflected wave. All these waves combined create an image.

The biggest problems when using ultrasound in organic media are the irregularities of the subject. How the wave behaves and propagates is difficult to predict since organic subjects often differ from one another creating difficulties in sorting out the echoing signals. The difference in the internal structure between healthy and contaminated trees should be enough to result in a noticeable difference in a signal sent through the tree stem.

### 3.2 Wave propagation and behavior in trees

The behavior of sound waves through the stem of the tree is dependent on the physical properties of the wood. The inner structure determines the path and the alteration of the wave when it passes through the wood. Due to the structure of the tree consisting of annual rings wood can be considered an orthotropic material, having different material properties in directions orthogonal to one another. Because of these physical properties of the wood, the wave travels faster in the grain than perpendicular to the rings. The sound waves are elastic due to the elasticity of the wood and can travel longitudinally or transversally.

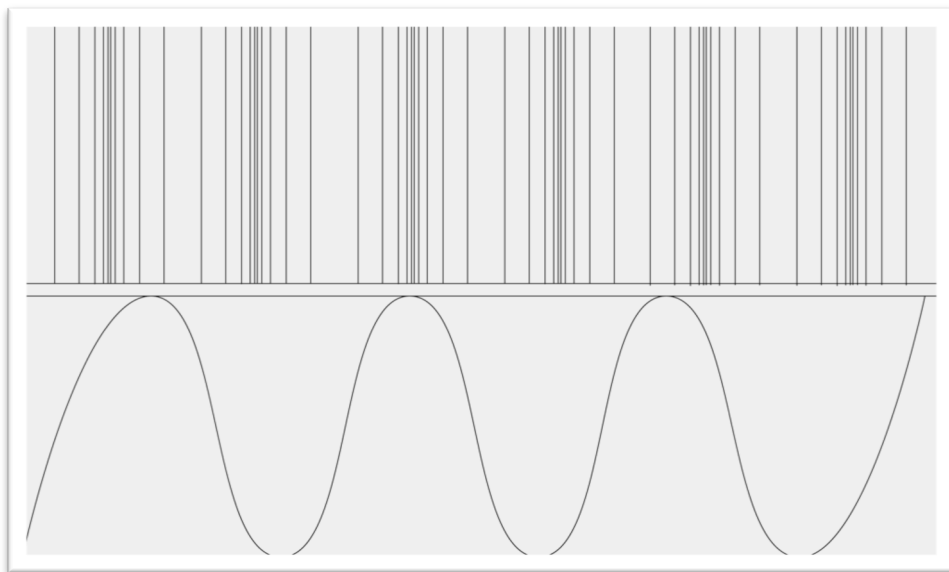


**Figure 2.1** *The top picture is an example of longitudinal waves and the lower one an example of a transverse wave.*

The longitudinal waves (P- waves) are primary waves that travel faster and create a pressure wave due to the alternating compression of the wave. The transversal waves are secondary waves (S-waves) that move through the body. They are also slower than the P-waves.

Decay in wood can affect the transmission time of the waves. The transmission time of waves in wood with rot increase notably. E.g. an increase of transmission time by 50 %, not uncommon in decayed wood, indicates decayed wood.<sup>15</sup>

When calculating the time of flight of the sound wave there is a significant difference between well conditioned wood and infected wood. In healthy wood the wave generally travels straight forward whilst a wave traveling in wood with rot will choose a path avoiding the decay, resulting in a longer lapse of time<sup>16</sup> (Figure 2.).

The attenuation of the signal is dependent on the path the sound wave travels. The signal is dampened more when it travels straight across the grain than when travelling along the grain.

### 3.3 Chirp

A chirp, or a frequency sweep, is a signal, which changes in frequency over time. The signal frequency can vary linearly or exponentially. The chirp is used to study which frequencies penetrate a subject most, creating a frequency fingerprint that describes the material.

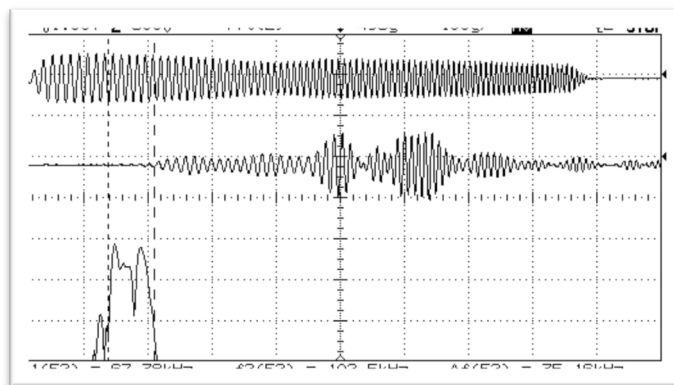


**Figure 3.2** The first curve from the top is an example of a linear chirp-signal. It alters in frequency over time. The second curve is the received signal and the third is the frequency spectrum.

15 X. Wang, F. Divos, C. Pilon, B. Brashaw, R. Ross & R. Pellerin, p. 3

16 X. Wang, F. Divos, C. Pilon, B. Brashaw, R. Ross & R. Pellerin, *Assessment of Decay in Standing Timber Using Stress Wave Timing Nondestructive Evaluation Tools*, U.S. Department of Agriculture, Forest Service, Forest Products Laboratory, Madison, WI. 2004. p 2

## 4 Method

The samples of wood were examined in several different ways in order to determine the sound waves behavior through the stem. The results were then analyzed to find out if the results could determine if the tree was contaminated with rot or not. The experiment does however not take into consideration to what degree of decay since this is irrelevant in forestry when thinning the forest. It is however of interest if decay in its initial stages can be detected.

### 4.1 Samples and their preparation

Our tree samples were from the Trolleholm estate, in southern Sweden. The samples of wood used in the measurements were either healthy or had a decay in its initial stages. They were both prepared in the same way by first removing the outer layer of bark, then shaving them the same size. The samples were all of ca. 40 cm in length and had a final diameter of ca. 20 cm. This length made the tree manageable for the equipment we used and was tall enough give alternation in the results height wise. The smooth surface was then varnished in order to seal in the dampness in the wood, knowing that the loss of it changes the wave propagation and thus alters the results significantly. If the wood would have been allowed to dry out it would probably crack and split altering the acoustic properties of the wood.

The samples were prepared in such a manner so they had the same prerequisites, however when working with natural materials it is impossible to create the exact same conditions. In this case knots and other irregularities may have affected the results for some measurements.



**Figure 4.1** *Tree sample with decay used in the thesis.*

## 4.2 Equipment and setup

The following equipment was used in the experiment:

- A pulse generator (HP 33120A) generating either a sinus wave of three cycles (Generator 1) or a linear chirp, with constant amplitude, (RC0612CT) depending on the type of measurement. 1Vp-p output. The generators frequency of 1,120 kHz gives the chirp signal a bandwidth of ca. 35 kHz, centered at 100 kHz.
- Burst rate 5/s for sinus signals, 3/s for chirp signals. Burst count for sinus signals was 3.
- Trig: internal
- An amplifier (RITEC, Gated pulse amplifier GA 2500) to amplify the signal. Ca. 500V output, drive ca. 8.
- A filter amplifier (Krohn-Hite Multichannel filter 3905B) creating low pass filter at 120 kHz and a high pass filter at 40 kHz. The signal is also amplified by 20 dB in both filters.
- Two acoustic exponential horns with piezoelectric transducers the signals were sent from one transducer and received by the other on the other side of the stem. The transducer used was of the type “Low Frequency Straight Beam Probe with Exponential Horn” from General Electric, Inspection Technologies. Product code 58769, frequency 100 kHz, relative bandwidth <50%.
- A digital Oscilloscope (HP 54600A) plots the reference signal directly from the filter as the signal sent in the wood and then plots the signal coming out of the wood.
- The results are then saved digitally on the computer for future analysis.



**Figure 4.2** *One of the exponential horns used in contact with the tree.*



**Figure 4.3** *One of the exponential horns used.*

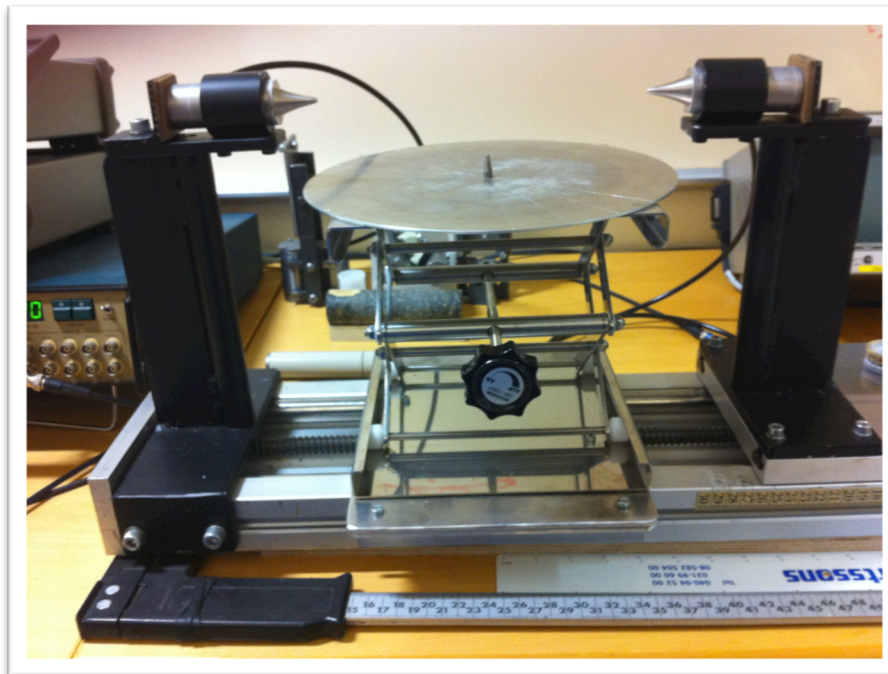


**Figure 4.4** *The set up used for the measurements. The tree specimen was placed on the circular plate and the exponential horns were fastened into the tree. For the reflection measurements the exponential horns were fastened both on the same side*

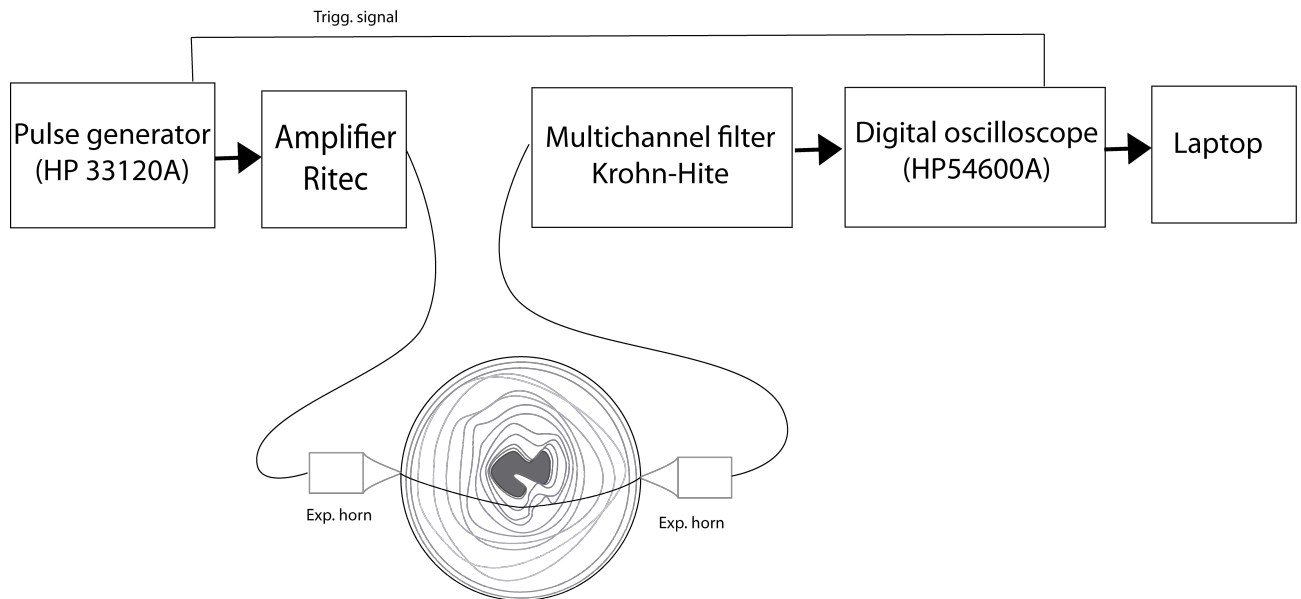


**Figure 4.5** *The entire laboratory setup.*

### 4.3 Measurement methods

The data for our analysis was measured in different ways. Two different signals were used, one of them a sinus-burst wave consisting of three cycles and the other one a chirp signal. For the sinus signal measurements the pulse generator was set to three cycles at a frequency of 100 kHz and the amplifier was set to 5-6 V. For the measurements using a chirp, the signal swept between the frequencies 73 and 126 kHz. The exponential horns were protected with a layer of tape to prevent the signal from travelling any alternative way apart from through the tree. Each measurement created a dent in the wood, to avoid these dents from affecting other results a single point was never used more than once. The dents were then covered to avoid the wood from drying. Since the wood is soft the probes needed to be tightened into the wood quite hard to create a good signal. Once a good signal was received the depth was recorded and used for all the other measurements.

Measurements were performed in three ways for the two different signals.

- Vertically. The wood was measured at points 2 cm apart along the 40 cm long specimen.
- Horizontally in the middle of the wood at three heights at approximately 18, 20 and 22 cm.
- Reflective measurements placing the two exponential horns on the same side of the wood.

In the future chapters the measurements using one frequency sinus wave are referred to as Series 1 and the measurements using chirp as Series 3. Series 2 and 4 contained the rotational and reflective results.

Later on Series 2 and 4 of the data were abandoned. The problem with the reflective measurements were that from the resulting signal it could be seen that the signal did not travel through the tree as we had wished, but taking the shortest path between the horns. The

rotational measurements were needed in order to make variance estimation. However these were not used later on.

## 5 Theory of spectral analysis

### 5.1 Statistical measures

A discrete stationary process can be written as  $\{X(t); t = 0, \pm d, \pm 2d \dots\}$  where  $X(t)$  is a random variable, sampled from a continuous-time signal, and  $t$  is the unit-sampling interval. This results in the sampling frequency of  $f_s = 1/d$ .

The expected value for a random variable  $X(t)$  is

$$m_X = E(X(t)), \quad (1)$$

and the variance is

$$V[X(t)] = E[(X(t) - m_X)^2] = E[X(t)^2] - m_X^2. \quad (2)$$

The covariance function for the stochastic process  $X(t)$  is given by

$$r_X(s, t) = C[X(s), X(t)]. \quad (3)$$

A stochastic process  $X(t)$  is called weakly stationary if the mean function  $m_X$  of the process is constant and the covariance function  $r_X(\tau)$  is finite and depends only on the time difference  $\tau = s - t$ <sup>17</sup>.

The correlation between two processes  $X(t)$  and  $Y(t)$  can be measured by the cross-covariance function and the correlation coefficient. Two independent variables are always uncorrelated, thus the correlation coefficient is  $\rho[X, Y] = 0$ , but two uncorrelated variables can still be dependent. The correlation coefficient is given by

$$\rho[X(t), Y(t)] = \frac{C[X(t), Y(t)]}{\sqrt{V[X(t)]V[Y(t)]}} \quad |\rho| \leq 1. \quad (4)$$

The correlation coefficient shows the linear co-variation between  $X(t)$  and  $Y(t)$ , and equals 1 if  $X(t)$  and  $Y(t)$  are perfectly linearly dependent.

### 5.2 Spectral analysis

The spectral analysis aims to model how the total power of a stationary process is distributed over frequency. It is a necessary tool in the application of stationary processes. The covariance function  $r_X(\tau)$  from (3) of a stationary process  $X(t)$  has a positive, integrable<sup>18</sup> and symmetric density function  $R(f)$ , defined on the open interval  $(-1/2, 1/2)$ , such as

$$r_X(\tau) = \int_{-1/2}^{1/2} e^{i2\pi f\tau} R_X(f) df, \quad (5)$$

where  $r_X(\tau)$  is a covariance function. The spectral density is given as the Fourier transform of  $r_X(\tau)$ ,

$$R_X(f) = \sum_{-\infty}^{\infty} e^{-i2\pi f\tau} r_X(\tau).$$

<sup>17</sup> G. Lindgren, H. Rootzén, M. Sandsten, *Stationary Stochastic Processes*, Lund University, 2009, p.41

<sup>18</sup> G. Lindgren, H. Rootzén, M. Sandsten, *Stationary Stochastic Processes*, Lund University, 2009, p.75

### 5.2.1 Linear filters and frequency function

A linear filter  $L$  is a transformation of the input function  $X(t)$  into the output function  $Y(t)=(LX)(t)$ . This relation can be written as  $Y(t)=S(X(t))$  where  $S$  is the system of transformation with the specification that it is linear and time invariant. Linearity means that  $S(ax_1 + bx_2) = aS(x_1) + bS(x_2)$  for all constants  $a$  and  $b$  and time invariant means that a time lag in the input signal, results in the same time lag in the output signal. The linear systems need also to be stable, meaning that a bounded input generates a bounded output.

Every linear, time invariant system  $S$ , has a function  $h(t)$ , called the *impulse response* of the system, defined as

$$Y(t) = S(X(t)) = \int_{-\infty}^{\infty} h(t-u)X(u)du = \int_{-\infty}^{\infty} h(u)X(t-u)du . \quad (6)$$

Every output  $Y(t)$ , from a linear, time-invariant system where the input  $X(t)$  is a stationary process, is also a stationary process. When a signal has passed through a system, it will be affected in a way, characteristic for the system. Both amplitude and phase will be affected and the affect is best defined by the *frequency function* of the system,  $H(f)$ .

$$H(f) = \sum_{u=-\infty}^{\infty} e^{-i2\pi f u} h(u), \quad \text{for } -1/2 < f < 1/2. \quad (7)$$

### 5.2.2 Cross spectrum

The cross-covariance function between two processes  $X(t)$  and  $Y(t)$  depends only on the time difference  $\tau = s - t$ . It measures the correlation between  $X(t)$  and  $Y(t)$ , as a function of time and is given by

$$r_{X,Y}(\tau) = C[X(s), Y(t)] = E[(X(t) - m_X)(Y(t) - m_Y)]. \quad (8)$$

The covariance matrix function is given by

$$\bar{r}_{X,Y}(\tau) = \begin{pmatrix} r_X(\tau) & r_{X,Y}(\tau) \\ r_{Y,X}(\tau) & r_Y(\tau) \end{pmatrix}. \quad (9)$$

As in the definition of spectral density in formula (5), the *cross-spectral density matrix* between  $X(t)$  and  $Y(t)$  can be written as

$$\bar{R}_{X,Y}(f) = \begin{pmatrix} R_X(f) & R_{X,Y}(f) \\ R_{Y,X}(f) & R_Y(f) \end{pmatrix}. \quad (10)$$

Using formula (7) above, the cross-spectral density between input and output signals can be written as

$$R_{X,Y}(f) = H(f)R_X(f), \quad (11)$$

where  $H(f)$  is the frequency function of the filter, as defined in formula (7).

In order to gain a physical interpretation of the relation between two signals, one can write the cross-spectral density in polar form

$$R_{X,Y}(f) = A_{X,Y}(f)e^{i\Phi_{X,Y}(f)}, \quad (12)$$

where  $A_{X,Y}(f) \geq 0$  is the modulus of  $R_{X,Y}(f)$ , called the cross-amplitude spectrum and  $0 \leq \Phi_{X,Y}(f) < 2\pi$  is the argument, called the phase spectrum. This enables us to define the *squared coherence spectrum*<sup>19</sup>.

$$\kappa_{X,Y}^2(f) = \frac{|R_{X,Y}(f)|^2}{R_X(f)R_Y(f)} = \frac{A_{X,Y}(f)^2}{R_X(f)R_Y(f)} \quad 0 \leq \kappa_{X,Y}^2 \leq 1. \quad (13)$$

### 5.3 The periodogram

The periodogram is a nonparametric method for estimating spectral density, also called power spectral density, of a dataset. In the definition of the periodogram, the Fourier transform of the data is used, according to formula (5) above. It can be computed for any frequency and it is periodic, with period one<sup>20</sup>.

$$R_X^*(f) = \frac{1}{n} \left| \sum_{t=0}^{n-1} X(t)e^{-i2\pi ft} \right|^2. \quad (14)$$

The periodogram is an estimate with large variance and bias, which needs to be reduced. Bias is reduced by *windowing* the data. The Hanning window, which is one of the most common, is written as

$$w(t) = \frac{1}{2} + \frac{1}{2} \cos\left(\frac{\pi t}{n}\right), \quad t = 0 \dots n-1. \quad (15)$$

Other possible methods include the Thomson multitaper and the Peak Matched Multiple Window methods<sup>21</sup>. These have the common property, which is the fact that they use different windows for different periodograms. Peak Matched Multiple Window methods aim to estimate a peak frequency optimally, by reducing variance as well as bias in that location. A multiple window spectrum is estimated as

$$R_X^*(f) = \frac{1}{K} \sum_{k=1}^K R_k^*(f) = \sum_{k=1}^K \left| \sum_{t=0}^{n-1} X(t)h_k(t)e^{-i2\pi ft} \right|^2, \quad (16)$$

where  $K$  is the number of periodograms that are used in the estimate. It is required that the periodograms are almost uncorrelated for a variance reduction. The number of windows  $K$  is approximately determined by the window length  $n$  and the band-width  $B$  of the spectral estimate

$$K \approx n \cdot B - 2.$$

<sup>19</sup> G. Lindgren, H. Rootzén, M. Sandsten, *Stationary Stochastic Processes*, Lund University, 2009, p.125

<sup>20</sup> G. Lindgren, H. Rootzén, M. Sandsten, *Stationary Stochastic Processes*, Lund University, 2009, p.180

<sup>21</sup> M. Hansson, G. Salomonsson, *A Multiple Window Method for Estimation of Peak Spectra*, 1997

## 6 Linear regression models

### 6.1 Simple regression

Two variables  $X$  and  $Y$  are measured and the aim is to find the linear relationship between these two. *Note that  $X$  and  $Y$  here do not refer to signals as in chapter 5, in this chapter they are variables in the regression model.* The dependent variable  $Y$  is assumed to be random with mean  $E[Y]$  and variance  $V[Y]$ . The simplest linear regression model for the observation  $Y_i$  that depends on  $X_i$  is given by

$$Y_i = \beta_0 + \beta_1 X_i + \varepsilon_i, \quad \varepsilon_i \in N(0, \sigma^2) \text{ for observations } i=1, 2, \dots, n, \quad (19)$$

where  $\beta_0$  is the intercept,  $\beta_1$  is the slope and the random errors  $\varepsilon_i$  are assumed normally distributed and pair wise independent<sup>22</sup>.

### 6.2 Multiple regression

The model from the previous section can be written in a generalized form, applicable for any number of independent variables  $X$ . Let  $p$  denote the number of independent variables and  $i$  the number of observations, then the formula (18) can be expanded and written as

$$Y_i = \beta_0 + \beta_1 X_{i1} + \beta_2 X_{i2} + \dots + \beta_p X_{ip} + \varepsilon_i, \quad \varepsilon_i \in N(0, \sigma^2) \quad (20)$$

In matrix notation the model is written as

$$\mathbf{Y} = \mathbf{X}\boldsymbol{\beta} + \boldsymbol{\varepsilon}$$

$$\begin{pmatrix} Y_1 \\ Y_2 \\ \vdots \\ Y_n \end{pmatrix} = \begin{pmatrix} 1 & X_{11} & X_{12} & \dots & X_{1p} \\ 1 & X_{21} & X_{22} & \dots & X_{2p} \\ \vdots & \vdots & \vdots & \ddots & \vdots \\ 1 & X_{n1} & X_{n2} & \dots & X_{np} \end{pmatrix} \begin{pmatrix} \beta_0 \\ \beta_1 \\ \vdots \\ \beta_p \end{pmatrix} + \begin{pmatrix} \varepsilon_1 \\ \varepsilon_2 \\ \vdots \\ \varepsilon_n \end{pmatrix} \quad \text{where } p' = p + 1,$$

$(n \times 1) \quad (n \times p') \quad (p' \times 1) \quad (n \times 1)$

Where  $\boldsymbol{\beta}$  is the vector with unknown constants, regression coefficients, that needs to be estimated from data. This model gives that  $\mathbf{X} \cdot \boldsymbol{\beta}$  is a vector including constant terms and  $\mathbf{Y}$  is a random vector which is the sum of the constant  $\mathbf{X} \cdot \boldsymbol{\beta}$  and the random vector  $\boldsymbol{\varepsilon}$ .

The variables  $\varepsilon_i$  are assumed to be independent and normally distributed random variables, which leads to  $Y_i$  being a normal random variable with mean  $\beta_0 + \beta_1 X_{i1} + \beta_2 X_{i2} + \dots + \beta_p X_{ip}$  and variance  $\sigma^2$  and  $Y_i$  are assumed independent of each other. This model relies on the assumption that  $\varepsilon_i$  are normally distributed, but even if this is not always true, one can still estimate  $\boldsymbol{\beta}$  with, the least square method, which is shown to be the best linear unbiased estimate<sup>23</sup>. The method aims to find  $\boldsymbol{\beta}$  that minimize the sum of squares,

<sup>22</sup> Rawlings, J.O., Pantula, S.G., Dickey, D.A.: *Applied Regression Analysis - A Research Tool*, 2ed, Springer, p.2

<sup>23</sup> Rawlings, J.O., Pantula, S.G., Dickey, D.A.: *Applied Regression Analysis - A Research Tool*, 2ed, Springer, p.77

$$Q(\beta_i) = \sum (Y_i - (\beta_0 + \beta_1 X_{i1} + \beta_2 X_{i2} + \dots + \beta_p X_{ip}))^2 = (\mathbf{Y} - \mathbf{X}\boldsymbol{\beta})'(\mathbf{Y} - \mathbf{X}\boldsymbol{\beta}) = \boldsymbol{\varepsilon}'\boldsymbol{\varepsilon}.$$

The solution needs to satisfy

$$\mathbf{X}'\mathbf{X}\hat{\boldsymbol{\beta}} = \mathbf{X}'\mathbf{Y},$$

which gives the estimated

$$\hat{\boldsymbol{\beta}} = (\mathbf{X}'\mathbf{X})^{-1} \mathbf{X}'\mathbf{Y}. \quad (21)$$

The estimated variance is  $\hat{\sigma}^2 = s^2 = \frac{\mathbf{e}'\mathbf{e}}{n-3}$  and  $s$  is the estimated standard deviation.

The residuals are derived from the observed values - predicted values, that is  $\mathbf{e} = \mathbf{Y} - \hat{\mathbf{Y}}$ .

The confidence interval for the expected value is given by  $E(Y_0) = \mathbf{x}_0\hat{\boldsymbol{\beta}}$

$$I_{E(Y_0)} = (\mathbf{x}_0\hat{\boldsymbol{\beta}} \pm t_{\alpha/2}(n-3)s\sqrt{\mathbf{x}_0(\mathbf{X}'\mathbf{X})^{-1}\mathbf{x}'_0}). \quad (22)$$

For comparing two data sets, one can choose to calculate the confidence interval for the difference in mean values, which is given by

$$I_{m_A - m_B} = ((m_A - m_B) \pm t_{\alpha/2}(n_A + n_B - 2)s\sqrt{\frac{1}{n_A} + \frac{1}{n_B}}) \quad (23)$$

Where the variance is given by

$$s^2 = \frac{\sum_{n_A} (x_{A,i} - m_A)^2 + \sum_{n_B} (x_{B,i} - m_B)^2}{(n_A + n_B - 2)} \quad (24)$$

### 6.3 Categorical variables

Categorical variables are used for representing non-numerical values in regression<sup>24</sup>. For example colors Red/Green or state of health for a tree, Healthy/Decay. A new variable is created for each category, e.g.

$$X_{healthy} = \begin{cases} 1 & \text{if } X_{state} = \text{Healthy} \\ 0 & \text{otherwise} \end{cases}$$

$$X_{decay} = \begin{cases} 1 & \text{if } X_{state} = \text{Decay} \\ 0 & \text{otherwise} \end{cases}$$

One of the categories can be used as reference for the model, e.g. the state Healthy, which gives us the regression model according to

$$Y_i = \beta_0 + \beta_1 X_{Decay,i} + \varepsilon_i.$$

One can use a categorical variable even if there are other variables in the same model, e.g. fitting a model with height  $X$ , as the independent variable and time as dependent variable  $Y$ . Considering two sets, which can be categorized by state of health, that is healthy or decay, one could try to fit a model, using the later as a categorical variable and height as a independent regular variable. The model can be described as,

$$Y_{Time,i} = \beta_0 + \beta_1 X_{Height,i} + \beta_2 X_{State,i} + \beta_3 X_{State \cdot Height,i} + \varepsilon_i, \quad (25)$$

where we have taken the state Healthy as a reference, meaning that

<sup>24</sup> Rawlings, J.O., Pantula, S.G., Dickey, D.A.: *Applied Regression Analysis - A Research Tool*, 2ed, Springer, p.289

$$X_{decay} = \begin{cases} 1 & \text{if } X_{state} = Decay \\ 0 & \text{otherwise} \end{cases}$$

Thus the coefficients  $\beta_2, \beta_3 \neq 0$  in the case of the state being Decay. They tell us how much the model must be adjusted from the reference state for the case of Decay.

## 6.4 Residual analysis

In all the regression models described in this chapter, it is assumed that the residuals are normally distributed, random and pair-wise independent. Studying the residuals from a model is essential for validation of the model, thus knowing how well the model is suited for the data. Among other studies, one can plot the residuals, which should then behave in a certain way.

When fitting a model to data, one wishes to see if there are any data points that are more influential than others, called outliers. These outliers are inconsistent with the rest of the data and can be shown as unexpectedly large residuals. When plotting the residuals versus the dependent variable  $X$ , this can be detected.

When plotting the residuals versus the predicted dependent variables  $\hat{Y}_i$ , one can see if the model has any structural inadequacies. In both cases, the residuals should look like random variation around zero.

The best model is not the one that explains as much of the variability as possible, but the one that explains as much as is practical.

## 7 Results from data analysis – Sinus measurements

### 7.1 The data

The measurements in Series 1 were done with a single frequency sinus wave as input signal. The analysis in this chapter aims to find the relation between the input and output signal, and how this relation differs from the healthy tree stock compared to the stock with decay.

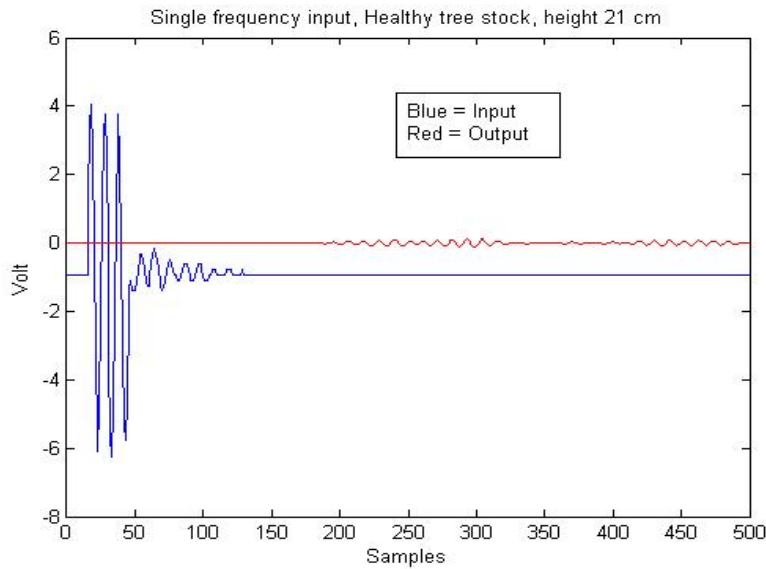


**Figure 7.1** Input and output signal from healthy tree stock at height 21 cm.

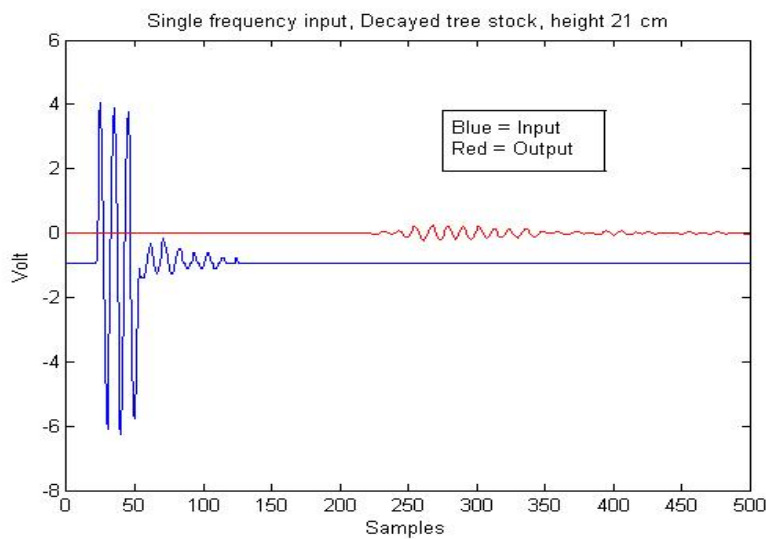


**Figure 7.2** Input and output signal from decayed tree stock at height 21 cm.

### 7.2 Energy analysis

In order to gain information about the signals relation to each other, one possible way is to compare the energies contained in the data. The energy ratio between two signals  $X(t)$  and  $Y(t)$  is determined with the formula below,

$$ER = \frac{\sum Y^2(t)}{\sum X^2(t)}. \quad (26)$$

The energy contained in the output signal  $Y(t)$  has thereafter been compared to the energy in the input signal  $X(t)$  for each measurement. The ratio between the output and input energies has been calculated and compared for the two data sets used in this study, that is the healthy and the decayed tree stocks. The aim is to get a perception of the attenuation of the signal by the system and find whether there is a significant difference between the two tree stocks or not.

In the figure below the energy ratios are shown and in the second figure we can see regression models for the two cases studied. The energy ratios are gathered in tables 10.1-10.2 in Appendix A. As seen in the regression model, the ratio between the energies increases with height for the decayed tree samples. This is expected, as the rot in the tree decreases with height, the ratio for the decay should approach the ratio for the healthy tree. The data shows a large variance, which affects the outcome.

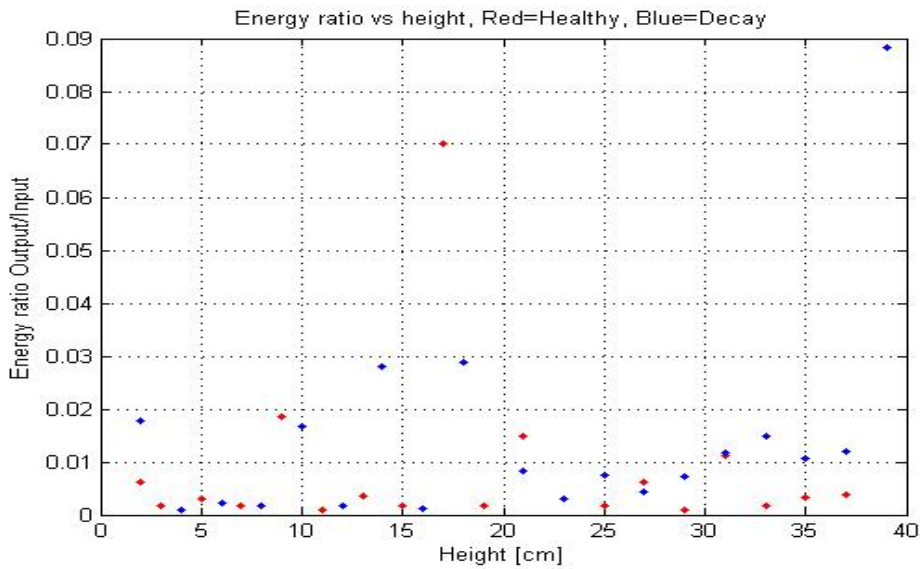


**Figure 7.3** The data, energy ratio for the output and input signal.

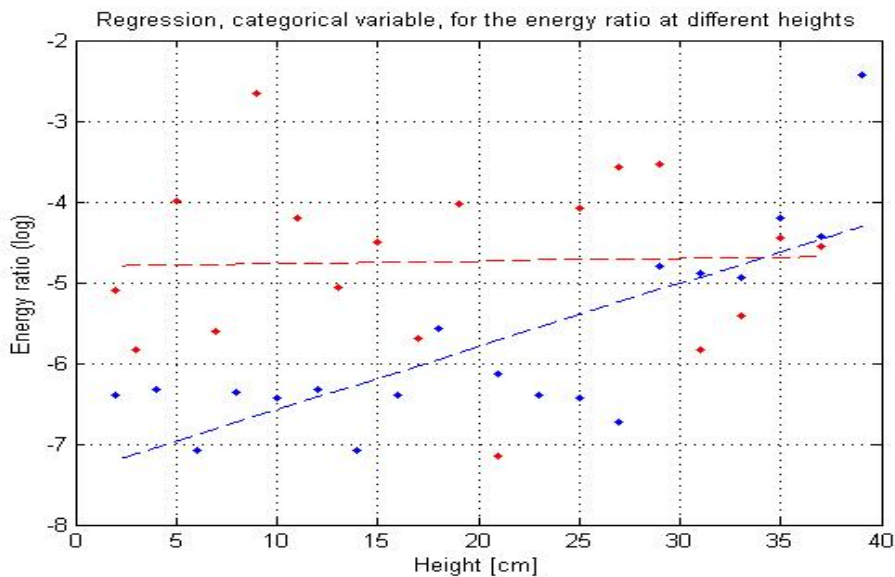


**Figure 7.4** Regression model for the energy ratio, red = healthy, blue = decay.

A regression model (Figure 7.4), with height and state (healthy / decay) as independent variables and the energy ratio as the dependent variable, has been determined. The state is used as categorical variable, according to formula (25). A confidence interval for the

difference in mean values has been calculated with the hypothesis

$$H_0 : m_{healthy} - m_{decay} = 0$$

$$H_1 : m_{healthy} - m_{decay} \neq 0$$

Using a 95 % confidence level gives the confidence interval

$$CI_{Energy\ ratio\ resies1} = [-0.0062 \quad 0.018]$$

This shows that the difference in mean is not significant. The means for ratios are  $m_{healthy} = 0.0144$  and  $m_{decay} = 0.0085$ . And the mean of the input-energy for healthy and decay are almost the same ( $m_{healthy}(Input) = 1.69$  and  $m_{decay}(Input) = 1.67$ ), which they should be, because it is the same input signal in both cases. Considering the means for the energy ratio, the interpretation of this is that a larger amount of the energy in the input signal passes through the healthy tree than the decayed tree. The decayed tree absorbs more of the input signal. However the difference in means is not sufficient for the confidence interval to give a significance difference.

### The residuals

The residuals are studied in order to validate the model, according to section 6.4. As seen in the plots below (Figure 7.5) we have an outlier in the data, which affects the result. Further analysis can be done, and another model can be fitted where the outlier is removed. The normal probability plot in figure 7.6 show that the residuals are almost normally distributed, which is desired, but not required, and since we are dealing with raw data from nature experiments, we find this model satisfactory.

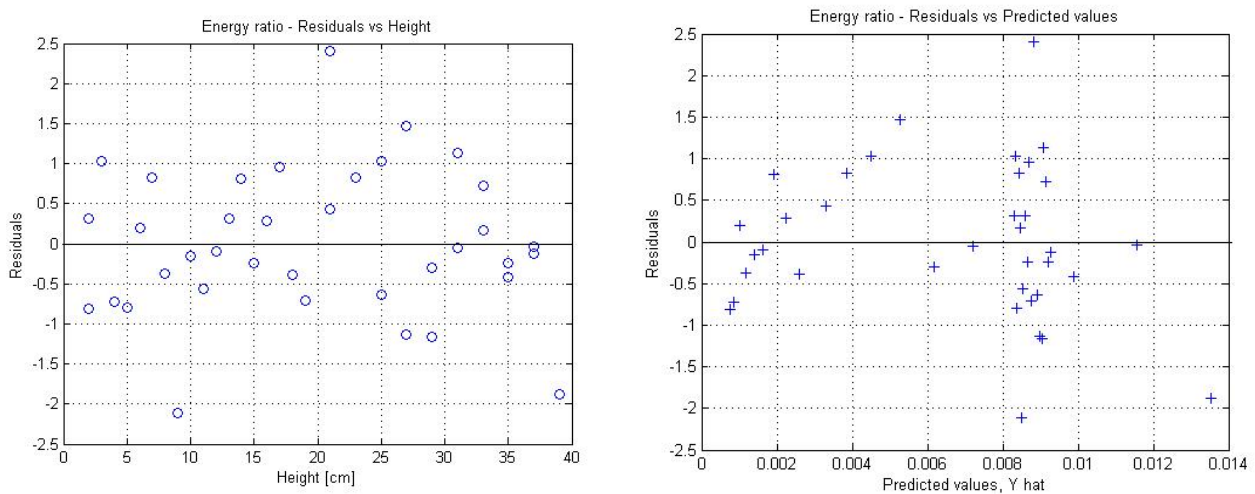


**Figure 7.5** a) Residuals versus height and b) residuals versus the predicted values for energy ratio.

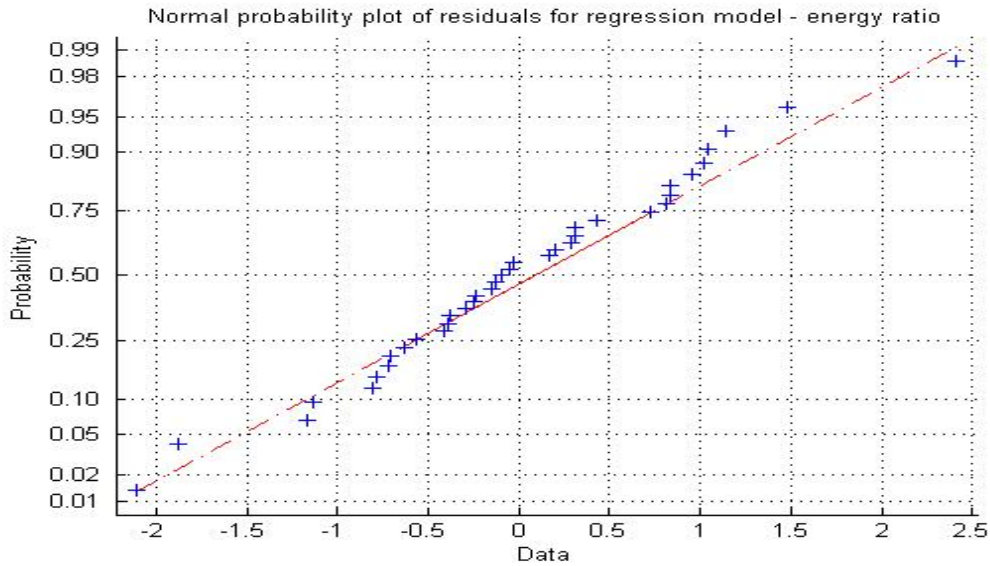


**Figure 7.6** Normal probability plot for energy ratio.

### 7.3 Velocity analysis

In this section the velocity at each measuring point has been calculated. This aims to determine whether there lays a significance difference in the sound velocity between the healthy and the decayed tree stock. The passing time for the signal is measured, that means, the signal passing through the tree stock. The diameter of each tree stock is known, as well as the time the sound takes, to pass through the two exponential horns. Thereafter the velocities are determined and shown in the figure 7.7 below. The velocities are found in Appendix A, tables 10.3-10.4.

The velocities for the signals are calculated as  $\frac{\text{The diameter}}{\text{Time of passage}} = \frac{m}{s}$ . (27)

In this case we only use the velocities in relative studies, therefore this is acceptable.

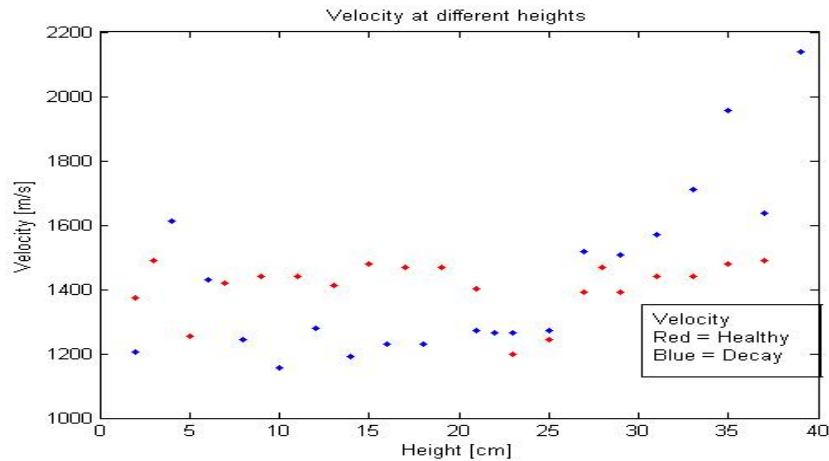


**Figure 7.7** Velocities for different height.

A 95 % confidence interval for the difference in mean is determined for the hypothesis,

$$H_0 : m_{healthy} - m_{decay} = 0$$

$$H_1 : m_{healthy} - m_{decay} \neq 0$$

The interval gives  $CI_{Velocity, series1} = [-102.9 \quad 153.6]$

This means that we cannot reject  $H_0$  at this confidence level. Therefore we cannot statically show that there is a difference between the velocity in the healthy and decayed tree. This is

however a very small study and a larger set of data could affect the outcome and perhaps show a different result. Two different regression models were used in this study, in order to the one best suited for this study. The first model, simple regression, as seen in figure 7.8, did not consider the health state of the tree, and as we can see, thus the fitted lines for the healthy and decayed data sets have the same slope but different intercepts. Suspecting that there must be a difference in the slope as well, a categorical variable was introduced in the next model. As seen in figure 7.9 the blue line that is fitted to the decayed data has a steeper slope, meaning that the velocity increases with height. The red line has a slope close to zero, meaning that the velocity in a healthy tree does not depend on the height. Possible other factors that affect the outcome are discussed in chapter 9.

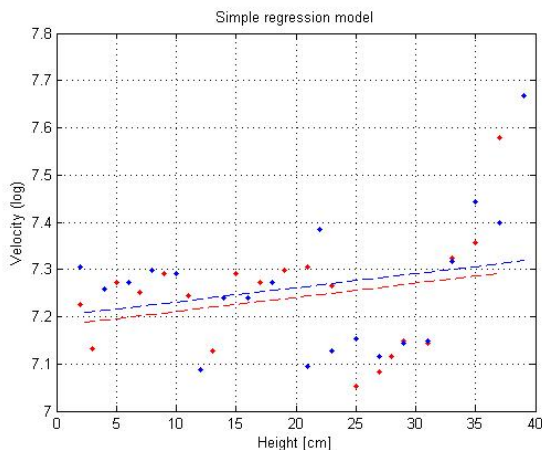


**Figure 7.8** Simple regression model.

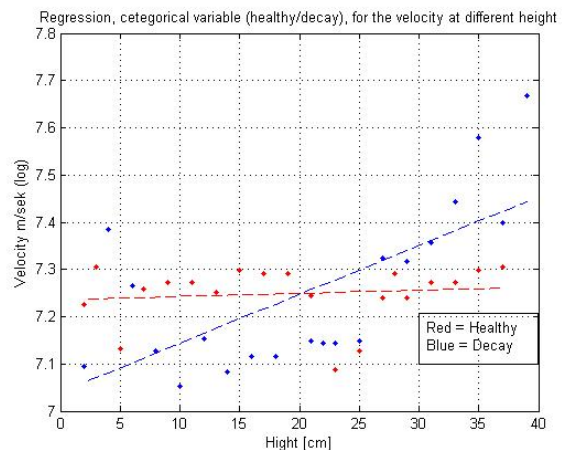


**Figure 7.9** Regression model with categorical variable.

### Residuals

The residuals in figures 7.10-7.11, in this regression model show no patterns, which means that the models fitted are suitable for this set of data. However the normal probability plot (Figure 7.12) shows that the residuals are not quite normally distributed in the second model, but more in the first model. This can be explained by the amount of independent variables which increased in the second model.

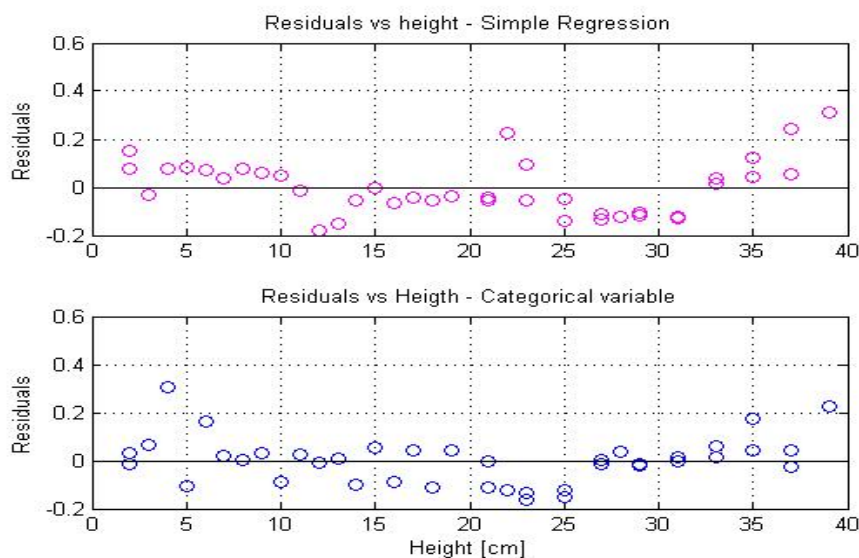


**Figure 7.10** Residuals vs height for the a) simple regression and b) for regression with categorical variable.

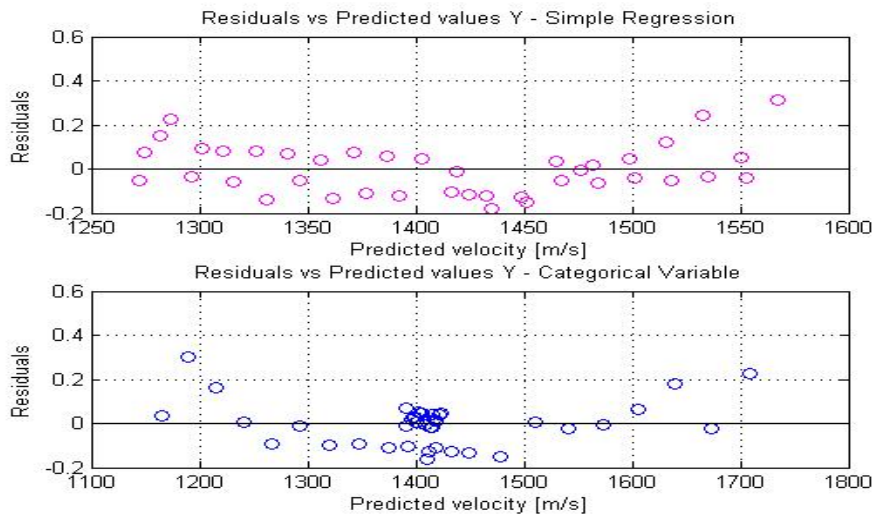


**Figure 7.11** Residuals vs predicted values for a) simple regression and b) regression with categorical variable.

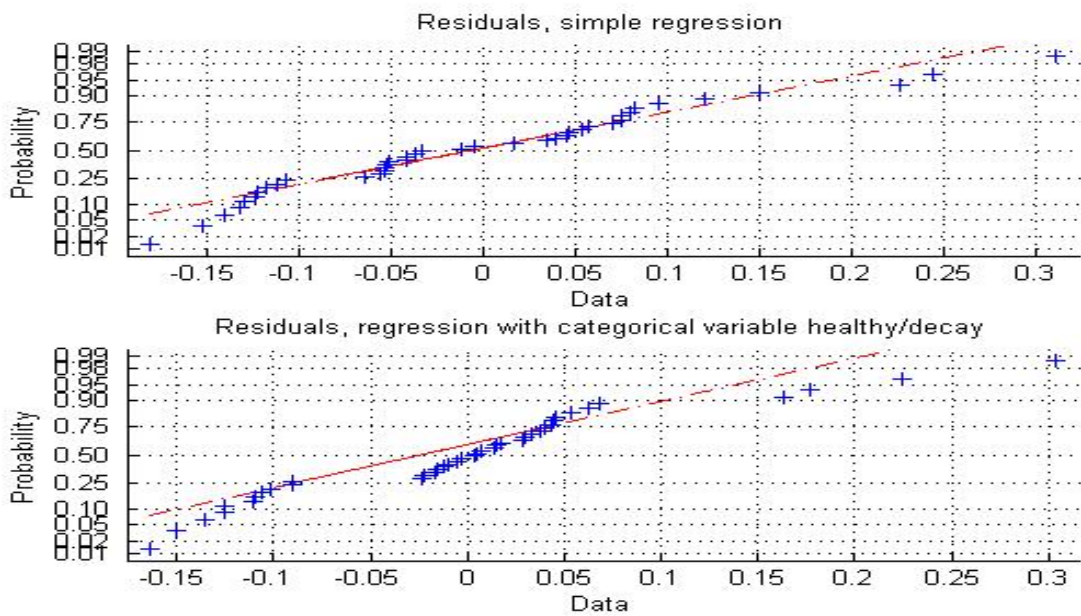


**Figure 7.12** Normal probability plots for the regression models, simple and with categorical variable.

## 8 Results from data analysis – Chirp measurements

### 8.1 The straight beam probe with exponential horn

All the signals were sent through the wood using an exponential horn with piezoelectric ceramics. The electrical signal is created in the pulse generator and then transformed into an acoustic signal. The signal travels through the wood, and is received on the other side. The signal is then once again transformed into an electrical signal. The horns resonance frequencies are 60 and 100 Hz. It is of interest to see how efficiently the chirp signal is transformed into an acoustic signal and back by simply studying the frequency distribution of the signal in two cases:

- The signal is sent through the two probes with their horns touching, peak to peak.
- The signal is sent through the two probes with a small piece of rubber in between the two horns.

#### 8.1.1 The reference input signal

The figure 8.1 below shows the chirp signal that was used as an input signal in Series 3. Figure 8.2 shows the spectrogram of this signal, where we can see the frequencies over which the signal sweeps. The spectral density for this signal has been plotted in order to get the frequencies and how the energy is distributed over the frequency-axis. As seen in figures 8.2-8.3 the frequencies are consistent.

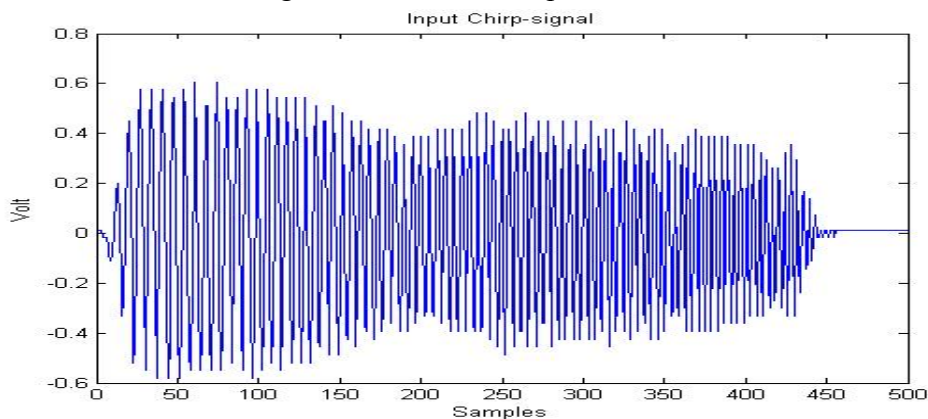


**Figure 8.1** The chirp signal used as input, after baseline adjustment.

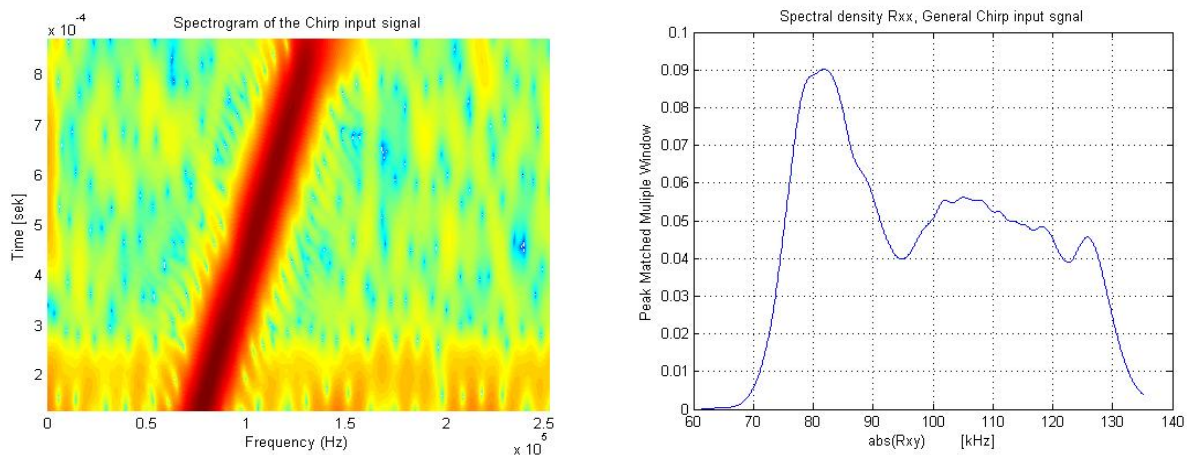


**Figure 8.2** The spectrogram of the input signal, in Series 3. The chirp sweeps over frequencies from 60-130 kHz.

**Figure 8.3** The spectral density of the input chirp signal.

### 8.1.2 Peak to peak

The chirp input signal has also been analyzed by studying its properties without any specimen between the exponential horns, sent peak to peak. As we can see in the spectrogram in figure 8.5 below, the frequency of the input signal varies between 60-130 kHz. The spectrogram of the output signal is weaker for higher frequencies, which means that the signal is slightly dampened for higher frequencies. The spectrogram shows the frequencies over which the signal sweeps, and the coherence function shows the amount of energy contained in these frequencies. As we can see they are consistent. In this measurement, it was concluded that the signal only passes through exponential horns, because if they were distant from each other, the signal would disappear.

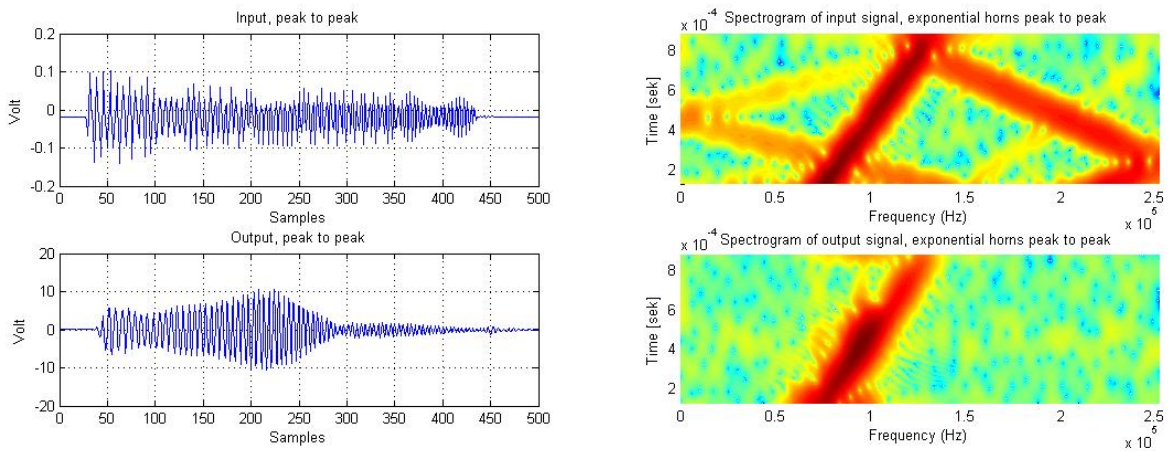


**Figure 8.4** The signal sent peak to peak of the exponential horns.

**Figure 8.5** The spectrogram of the input and output chirp signal, sent through the exponential horns, when they are put peak to peak.

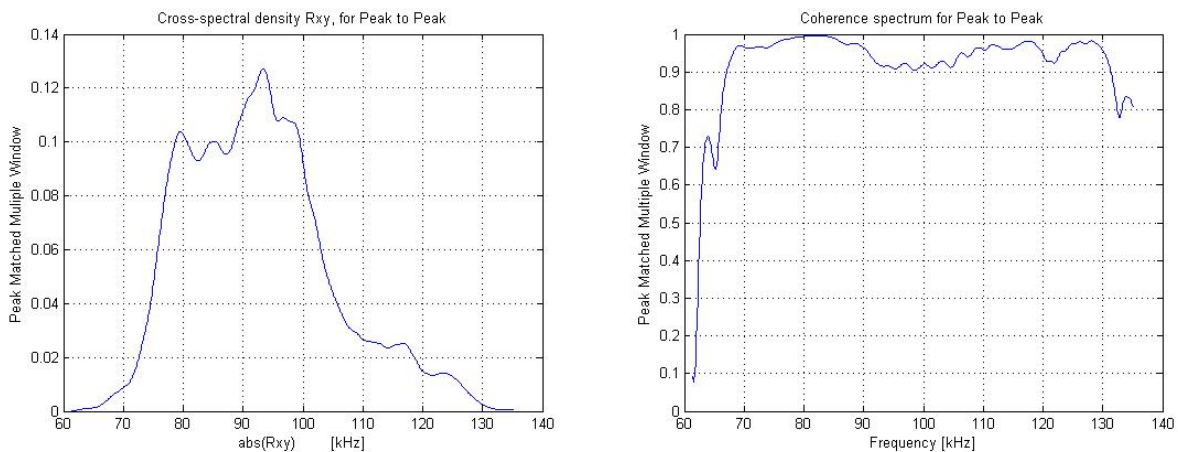


**Figure 8.6** The cross-spectral density between the chirp input and output signals sent through the exponential horns.

**Figure 8.7** The coherence spectrum of the signals sent peak to peak.

### 8.1.3 Peak to rubber

Another experiment was done; where the chirp signal was sent through the exponential horns with a little rubber blanket (1 mm) in between. This did not affect the signal significantly, which can be seen by comparing the figures from the previous section with figures 8.8-8.9.

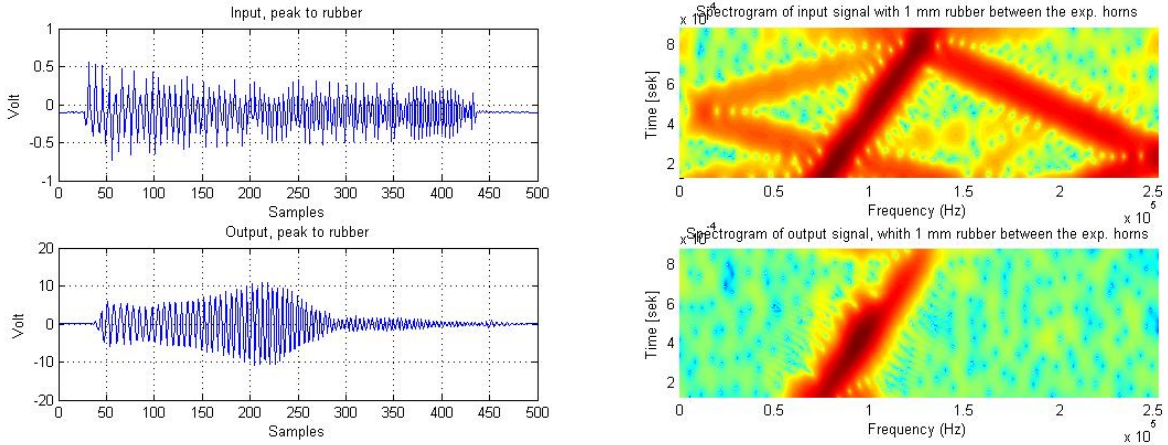


**Figure 8.8** The signal sent through 1 mm rubber, input and output.

**Figure 8.9** The spectrogram of the chirp signal, input and output, sent through the exponential horn, with 1 mm rubber in between.

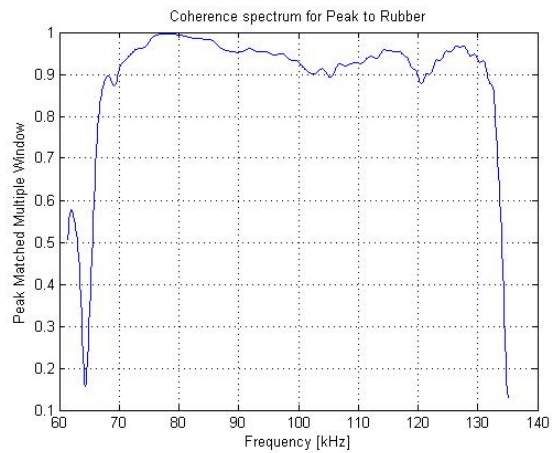
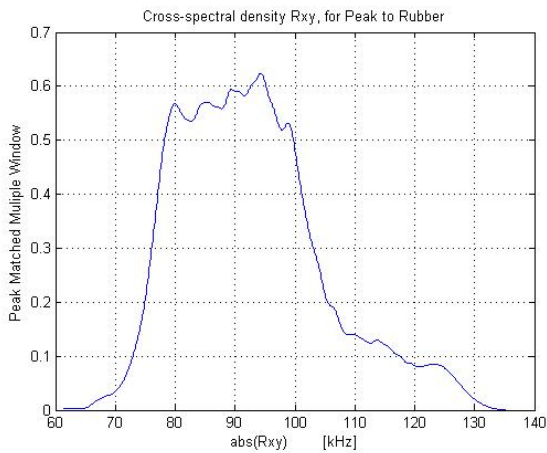


**Figure 8.10** The cross-spectral density between the chirp input and output signals sent through the exponential horns.

**Figure 8.11** The coherence spectrum of the signals sent through the exponential horns with 1 mm rubber in between.

## 8.2 Data alignment

The data sampled from Series 3 showed a strange symmetric pulse, as seen in Figure 8.13, which was not shown in the oscilloscope. Assuming that this is a coding error, it is necessary to be removed from our original data. This has been done by an averaging algorithm shown in the figure 8.12 below. The result is shown in figures 8.13-8.15.

$$\begin{aligned} &2 \leq x(i) \leq x(n-2) \quad n = 500 \\ &\text{if } x(i) = \min(X) \text{ and } x(i+1) = \min(X) \\ &\quad x(i) = \frac{2x(i-1) + x(i+2)}{3} \quad \text{and} \quad x(i+1) = \frac{x(i-1) + 2x(i+2)}{3} \\ &\text{else} \\ &\quad x(i) = \frac{x(i-1) + x(i+1)}{2} \end{aligned}$$

**Figure 8.12** This algorithm was used to remove the coding error found in the data.

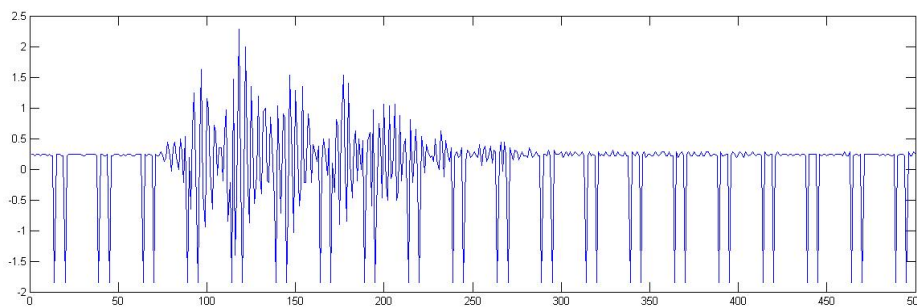


**Figure 8.13** The original output signal

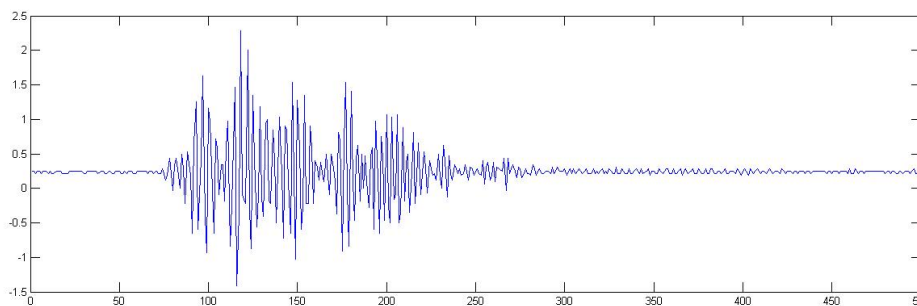


**Figure 8.14** Signal after error correction

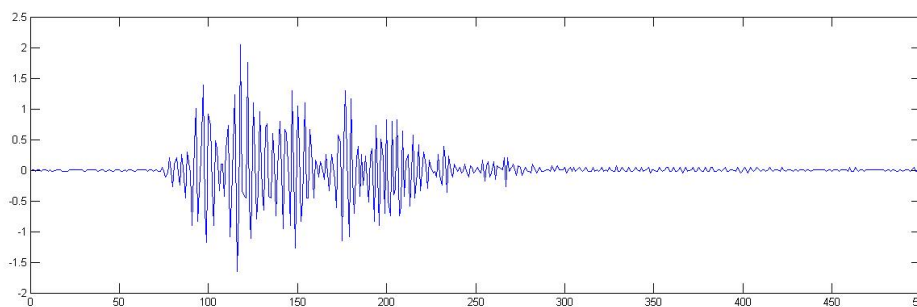


**Figure 8.15** Signal after baseline alignment

The correction above did not prove to be suitable for the input signal, due to large information loss. However it did not change the output signal in the same proportion, therefore every output signal could be corrected before analysis. A reference signal, that did not show the same error and that did not need correction was used as the input. However it did need baseline adjustment. The chirp-signal used as the input  $X(t)$  is shown in the figure below.

The output signals were resampled in order to get same sampling frequency as the input signal. This resulted in the two signal arrays having different lengths, which also needed to be corrected. Figure 8.16 shows the input signal and the corrected, resampled output signal for height 11 cm, for the healthy tree stock.

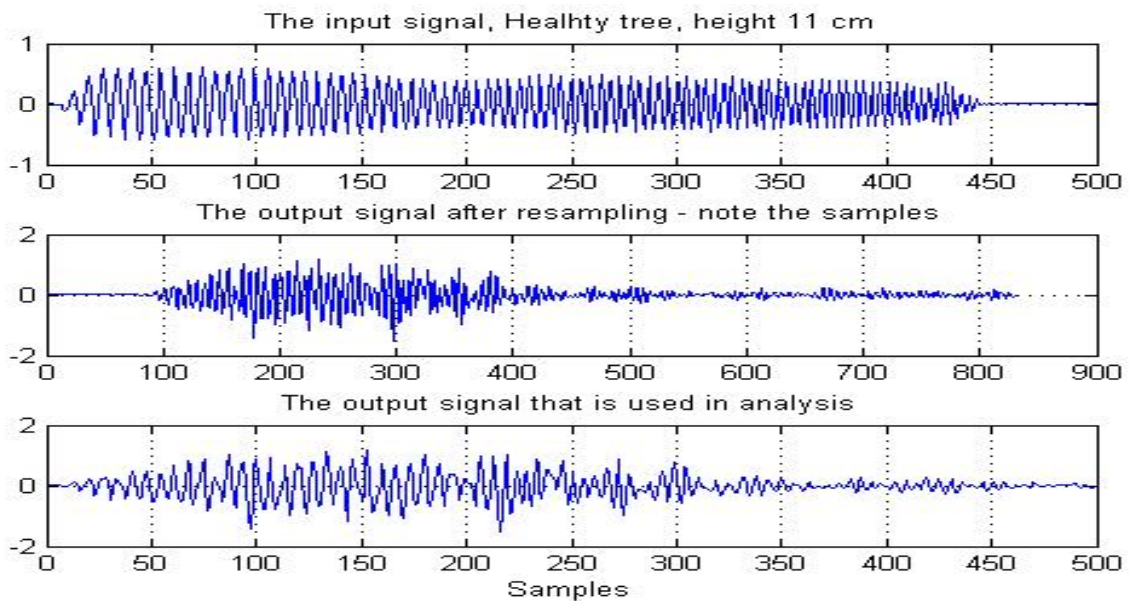


**Figure 8.16** The input and output signal for the healthy tree stock, at height 11 cm.

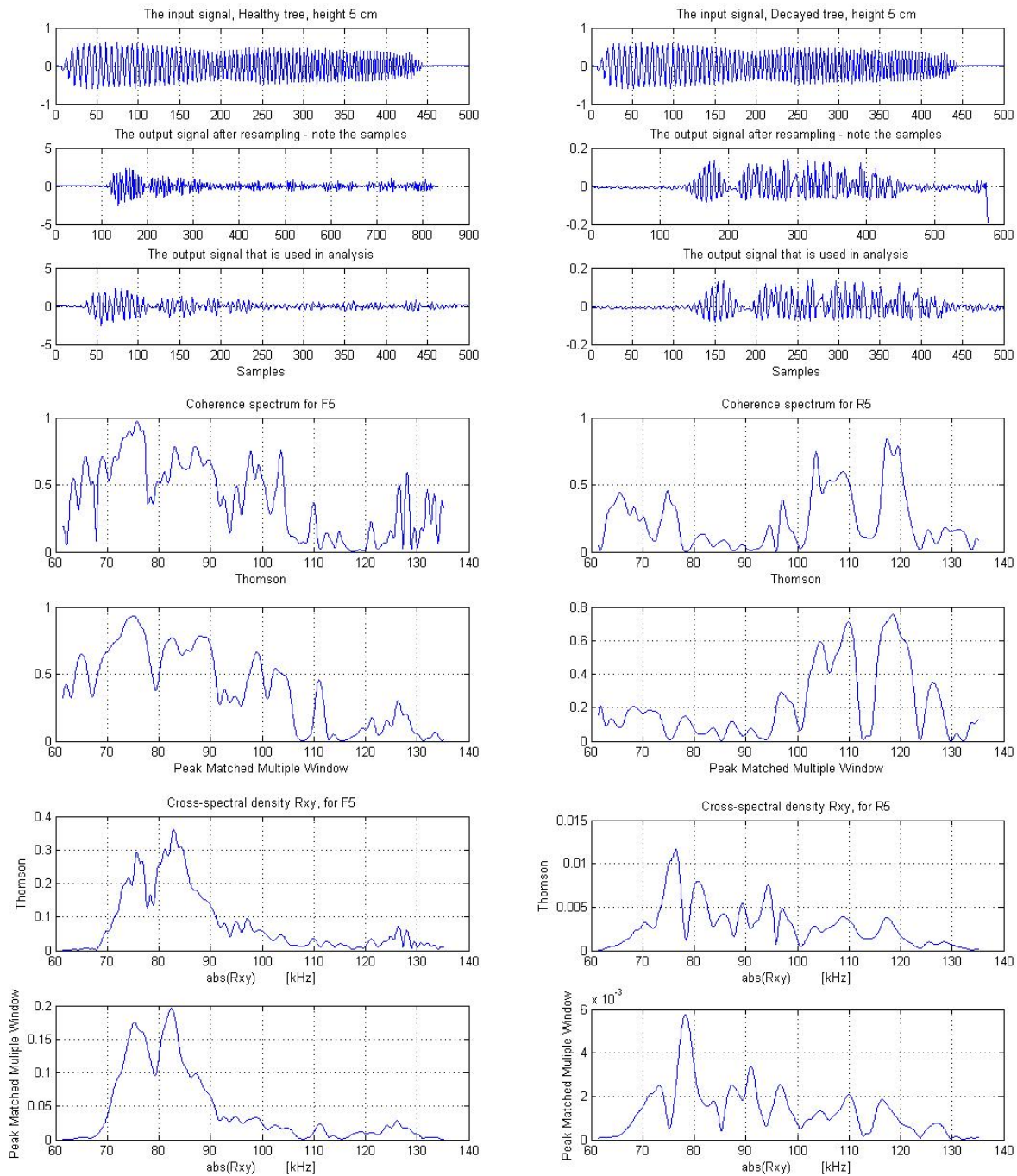
### 8.3 Frequency analysis

In the frequency and spectral analysis below, a general input signal, as shown in figure 8.1 has been used. The output signal is taken from 16 measuring points in each tree stock, that is one healthy and one decayed tree stock.

The coherence function from formula (12) in section 5.2.1 has been determined for the input-output relation at these 16 points. This has been done by determining the spectral and cross-spectral density for the input and the output signals specifically.

In order to reduce variance and bias, windowing methods according to Section 5.3 have been used. The Thomson multitaper method with  $K=4$  windows and the Peak Matched Multiple windows with  $K=8$  windows are the two methods chosen. The number of windows is chosen based on former studies<sup>25</sup> and empirical results. The coherence function has been plotted for each height, for the relevant frequency interval 60-135 kHz.

<sup>25</sup> M. Hansson, G. Salomonsson, *A Multiple Window Method for Estimation of Peak Spectra*, 1997

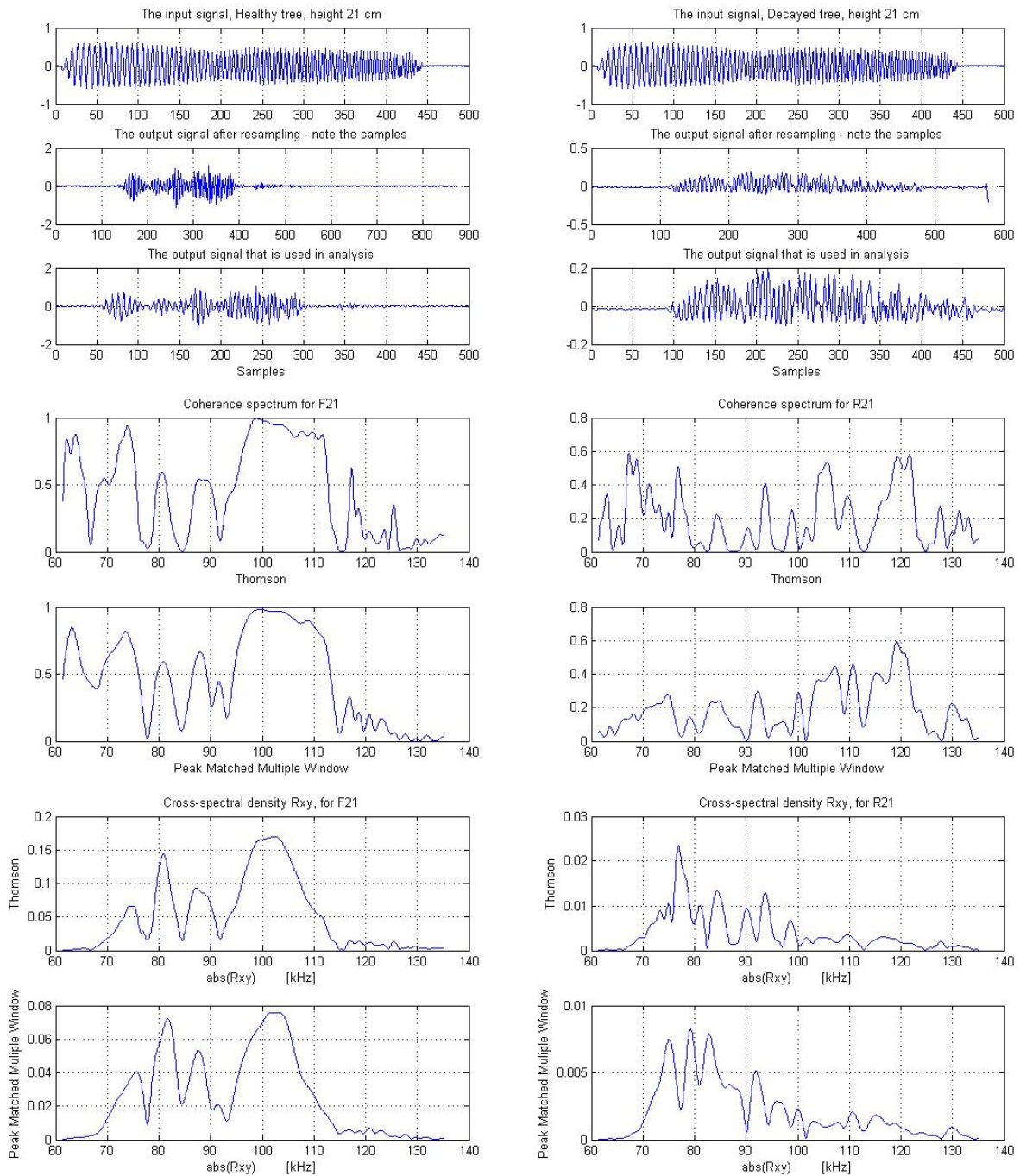


**Figures 8.17-8.18** The signal from one healthy and one decayed specimen, at the height 5 cm. Both figures show how the signals were corrected and resampled in order to get the same sampling frequency as the input chirp signal.

**Figures 8.19-8.20** The coherence spectrum for the two specimens (healthy and decayed) at height 5 cm, calculated with the two methods Thomson's Method and Peak Matched Multiple Windows Method. We can see that a higher amount of the energy is located in the first half of the spectrum for the healthy tree, compared to the decayed.

**Figures 8.21-8.22** The cross-correlation between the input and output signals from the two specimens (healthy and decayed) at height 5 cm.

Note: F5 refers to the healthy specimen at height 5 cm, F meaning Frisk = Healthy (Swe) R5 refers to decayed specimen at height 5 cm, R meaning Röta = Decay (Swe)

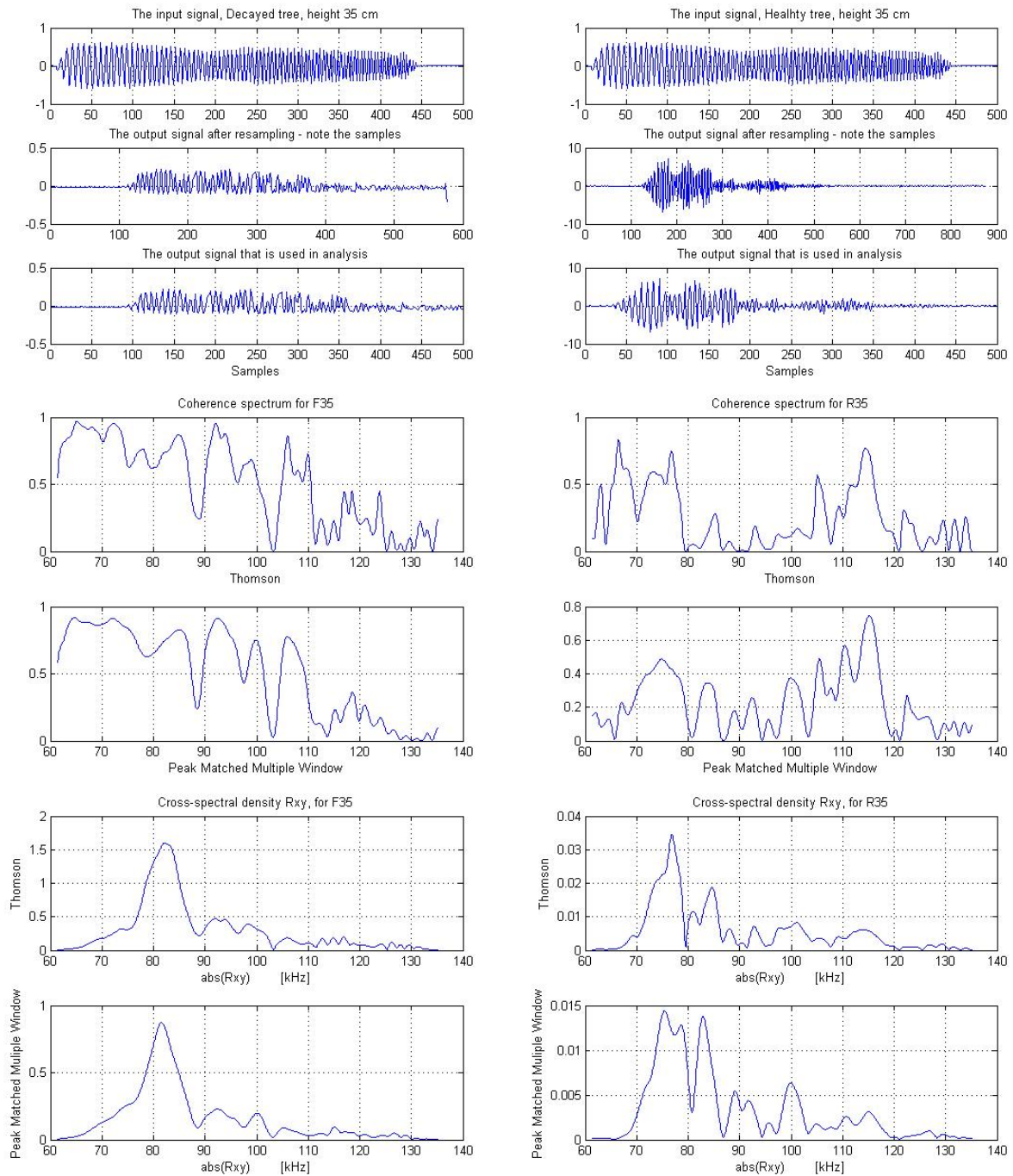


**Figures 8.23-8.24** The signal from one healthy and one decayed specimen, at the height 21 cm (middle of the specimen). Both figures show how the signals were corrected and resampled in order to get the same sampling frequency as the input chirp signal.

**Figures 8.25-8.26** The coherence spectrum for the two specimens (healthy and decayed) at height 21 cm, calculated with the two methods Thomsons Method and Peak Matched Multiple Windows Method. We can see that a higher amount of the energy is located in the first half of the spectrum for the healthy tree, compared to the decayed.

**Figures 8.27-8.28** The cross-correlation between the input and output signals from the two specimen (healthy and decayed) at height 21 cm.

Note: F21 refers to the healthy specimen at height 21 cm, F meaning Frisk =Healthy (Swe) R21 refers to decayed specimen at height 21 cm, R meaning Röta =Decay (Swe)



**Figures 8.29-8.30** The signal from one healthy (F35) and one decayed (R35) specimen, at the height 35 cm (top end of the specimen). Both figures show how the signals were corrected and resampled in order to get the same sampling frequency as the input chirp signal.

**Figures 8.31-8.32** The coherence spectrum for the two specimens (healthy and decayed) at height 35 cm, calculated with the two methods Thomsons Method and Peak Matched Multiple Windows Method. We can see that a higher amount of the energy is located in the first half of the spectrum for the healthy tree, compared to the decayed.

**Figures 8.33-8.34** The cross-correlation between the input and output signals from the two specimen (healthy and decayed) at height 35 cm.

Note: F35 refers to the healthy specimen at height 35 cm, F meaning Frisk =Healthy (Swe) R35 refers to decayed specimen at height 35 cm, R meaning Röta =Decay (Swe)

### 8.3.1 Coherence spectrum analysis in two intervals

The analysis aims to determine the coherence contained in the first half of this interval, for the healthy and decayed tree. The intervals used are:

$$61 \leq I_1 \leq 98 \text{ kHz}$$

$$98 < I_2 \leq 135 \text{ kHz}$$

In this study we aim to determine the coherence at different frequency intervals. For example, determining the coherence ratio ( $CR$ ) between the interval  $a \leq I \leq b - n \text{ kHz}$  and the total frequency  $a \leq I \leq b \text{ kHz}$  is done by a simple summation.

$$CR = \frac{\frac{1}{b-n} \sum_a^{b-n} \kappa_{X,Y}(f)}{\frac{1}{b} \sum_a^b \kappa_{X,Y}(f)} \quad (28)$$

The probabilities for each coherence spectrum have been determined using formula (16). With the use of tables 10.5-10.6 Appendix A, a linear regression model has been calculated, according to the regression model in (17), section 6.1. The regression model was used to calculate a confidence interval for the difference in mean for the hypothesis below. The confidence is level  $1 - \alpha = 95\%$ . The determined mean ratios measured with the Thomson Method are  $m_{healthy,Tho} = 0.696$  and  $m_{decay,Tho} = 0.430$ . And with Peak Matched Multiple Windows they are  $m_{healthy,PMMW} = 0.702$  and  $m_{decay,PMMW} = 0.361$ .

$$H_0: m_{healthy} - m_{decay} = 0$$

$$H_1: m_{healthy} - m_{decay} \neq 0$$

The confidence intervals for both methods show that  $H_0$  can be rejected at this significance level, though they are:

$$CI_{ratio,Tho} = [0.1906 \quad 0.3409]$$

$$CI_{ratio,PMMW} = [0.2691 \quad 0.4139]$$

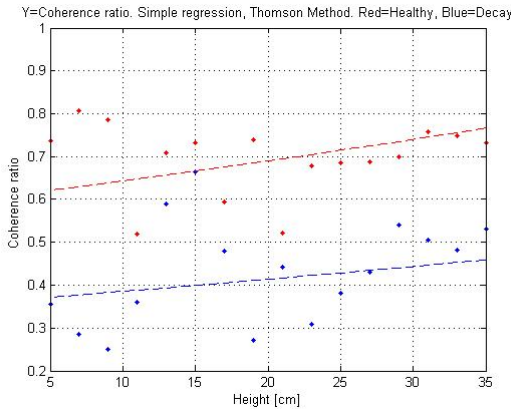


**Figure 8.35** Regression model for the coherence ratio contained in interval 1, where the coherence spectrum is determined with the Thompson Method.

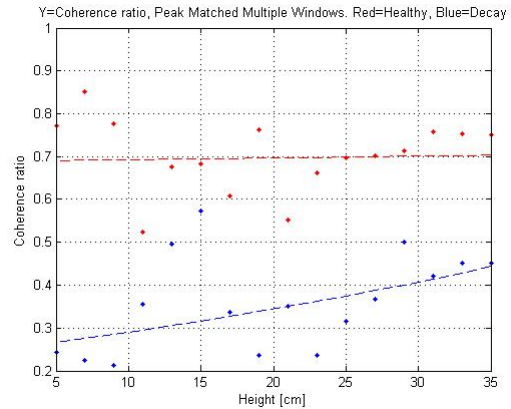


**Figure 8.36** Regression model for the coherence ratio contained in interval 1, where the coherence spectrum is determined with the Peak Matched Multiple Windows Method.

### Residual analysis

In this part we have analyzed the residual from the regression done for the Peak matched multiple windows method. This is a more refined method that is proven to be more accurate than the Thomson method<sup>26</sup>. The regression model used for the Thompson method will not be analyzed further.

The residuals are plotted against the height, and we can see in figure 8.37 they show no pattern and we can assume that the model fitted to the data from Peak matched multiple windows method is suitable. However they do not behave like normally distributed residuals, which is questionable. The variance in the data is large which can partly explain this phenomenon. This is a result of the interval for which the energy ratio is calculated, being large, 50% of the total coherence spectrum.

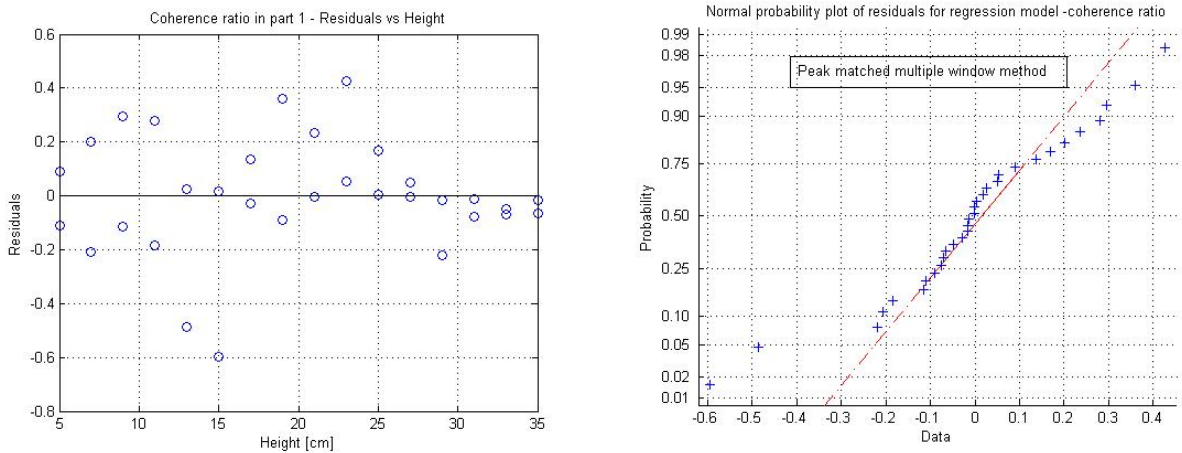


**Figure 8.37** The residual plotted against the height from the regression model (Peak Matched Multiple Windows Method).

**Figure 8.38** Normal probability plot for the regression model shows how close to normally distributed the residuals are.

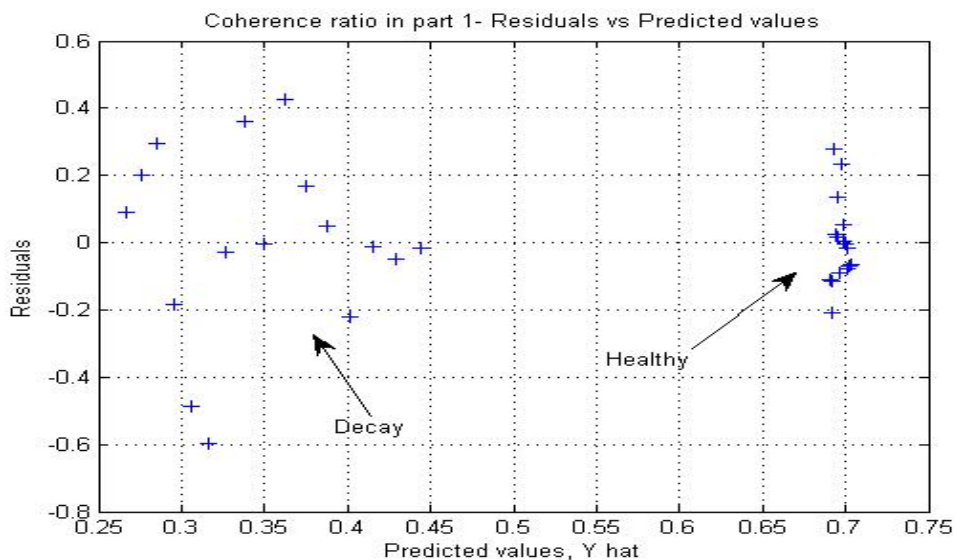


**Figure 8.39** The residuals plotted against the predicted values. Two groups are shown, for data from the healthy and the decayed sets.

<sup>26</sup> M. Hansson, G. Salomonsson, *A Multiple Window Method for Estimation of Peak Spectra*, 1997

### 8.3.2 Coherence spectrum analysis in three intervals

From the previous section we could conclude that there is a significance difference in the mean energy contained in the first interval of the coherence function, the interval being  $61 \leq I_1 \leq 98 \text{ kHz}$ . This is however a large interval and our aim are to decrease this interval further. This is done by portioning the coherence spectrum in three equal parts and determining the energy ratio of the middle part for each measuring point and thereafter comparing the data from healthy and decayed. The middle part is where the most interesting frequencies are contained, which will be our area of focus. The coherence spectra could of course be portioned even smaller intervals, but it was decided that in order to decrease the information from the coherence spectrum, three parts would be sufficient. The intervals are

$$61 \leq I_1 < 85 \text{ kHz}$$

$$86 \leq I_2 \leq 112 \text{ kHz}$$

$$112 < I_3 \leq 135 \text{ kHz}$$

In this part, only the Peak Matched Multiple Windows Method is used and we only calculate the coherence contained in interval 2. A regression model is fitted to data, according to formula (25) and the same hypothesis has been used, as in the previous part 8.3.1. The mean values for the energy ratio for interval 2 are  $m_{healthy} = 0.4448$  and  $m_{decay} = 0.3413$ . A 95 % confidence interval, as seen below, gives that we can reject  $H_0$  meaning that there is significant difference in the mean values. The energy ratio from healthy data is significantly higher than from decayed data.

$$CI_{I_2, PMMW} = [0.0525 \quad 0.1544]$$

Looking at the residuals in figure 8.42, it can easily be concluded that they are almost perfectly normally distributed and random.

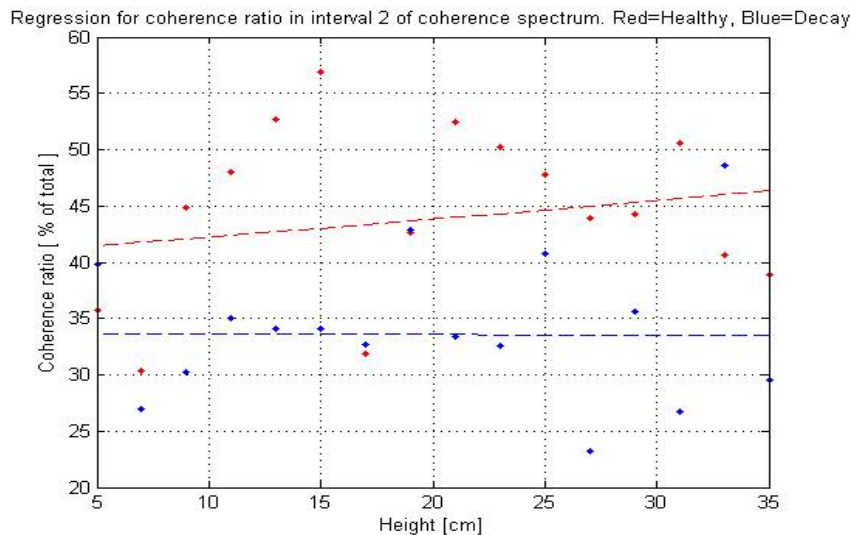


**Figure 8.40** The regression model for the coherence ratio contained in the interval  $I_2$  of the coherence spectrums.

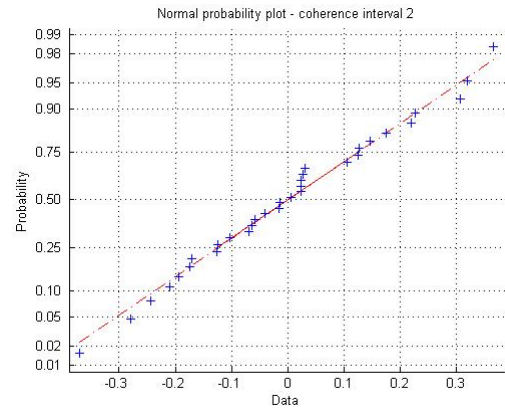
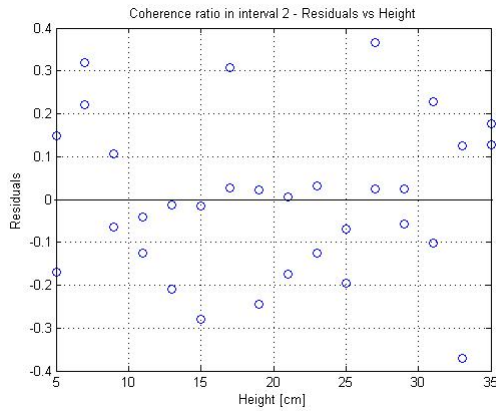


**Figure 8.41** The residuals plotted against height. No patterns are shown.

**Figure 8.42** Normal probability plot of residuals. Almost perfectly normally distributed.

## 8.4 Energy analysis

A simple analysis concerning the amount of energy contained in the signals measured has been done. In this study the original input signals have been used for each height and tree stock. They have initially been corrected according to the method described in Table 7.1. The energy ratio between the input and output has therefore been calculated and a simple regression model has been applied. The ratios and energies can be found in Appendix. In order to determine if there is a significant difference in the mean ratios, a confidence interval has been calculated for the hypothesis below.

$$H_0 : m_{healthy} - m_{decay} = 0$$

$$H_1 : m_{healthy} - m_{decay} \neq 0$$

The determined mean ratios are  $m_{healthy} = 0.103$  and  $m_{decay} = 0.004$ .

The confidence level  $1 - \alpha = 95\%$  and the confidence interval give the result

$$CI_{Energy\ ratio} = [0.0026 \quad 0.1753]$$

This means that we can reject  $H_0$  at the significance level 95 %, thus there is a difference in the energy mean ratios between the healthy and decayed tree samples. This means that the energy contained in the output signals is significantly higher in the healthy tree compared to the decayed tree.

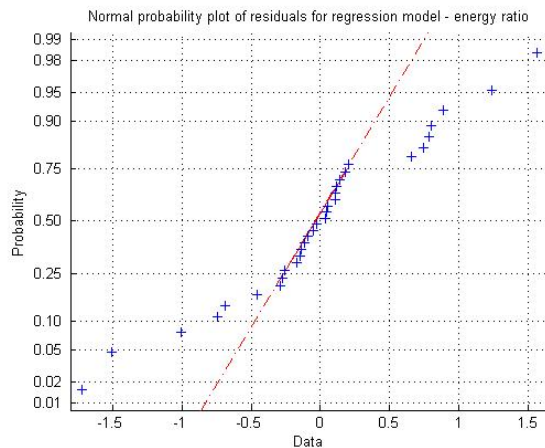
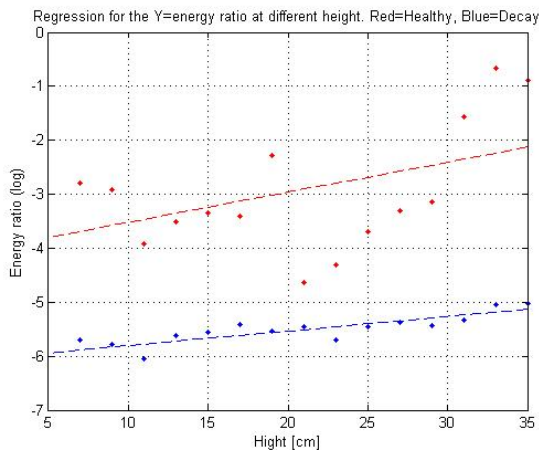


**Figure 8.43** The regression model for the energy ratio.

**Figure 8.44** The normal probability plot for the residuals from the regression model for the energy ratio contained in the output signal, compared to input

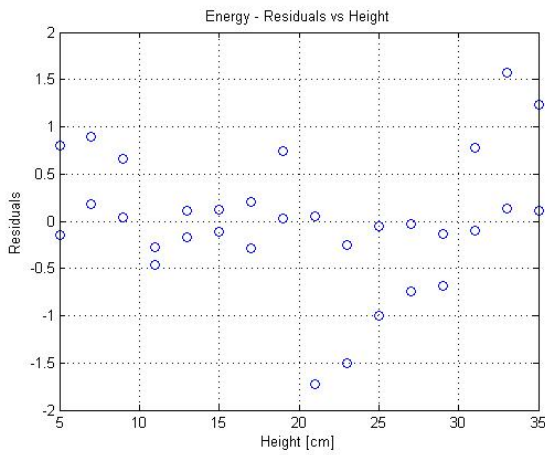


**Figure 8.45** Residuals plotted against height.

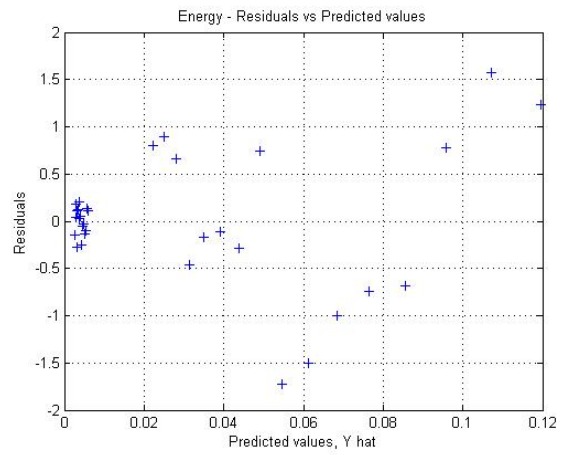


**Figure 8.46** Residuals plotted against predicted values.

## 8.5 Velocity analysis

The studies done in this thesis contain time measurements for the signal at different heights for healthy and decayed tree stocks. The time measured is the crossing time for the input signal. In the calculations below, the time for the signal to pass through the exponential horns, has been subtracted and therefore the velocity has been calculated. The values can be found in Appendix.

A regression model for the velocity has been calculated, with height and state, meaning healthy or decay, as independent variables. The state has been used as a categorical variable, according to section 6.3 and a confidence interval for the mean velocity in healthy and decayed tree has been determined for the hypothesis:

$$H_0 : m_{healthy} - m_{decay} = 0$$

$$H_1 : m_{healthy} - m_{decay} \neq 0$$

The determined mean ratios are  $m_{healthy} = 1573$ ,  $m_{decay} = 1221$  and the confidence interval with the confidence level 95 % gives:

$$CI_{Velocity} = [272.7 \quad 431.7]$$

This shows that  $H_0$  can be reject at this confidence level, meaning that there leys a significant difference in the mean values for the velocity in healthy and decayed tree stocks.

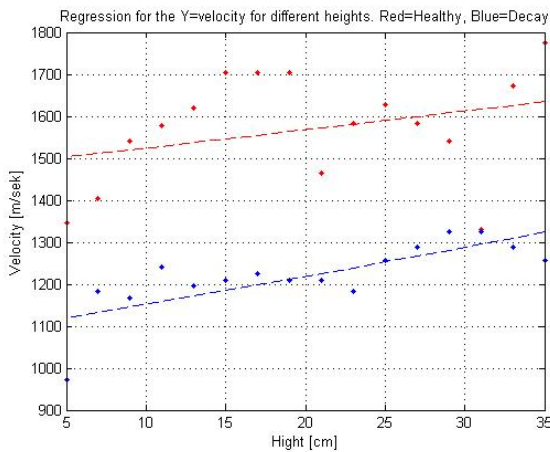


**Figure 8.47** Regression model for the velocity.

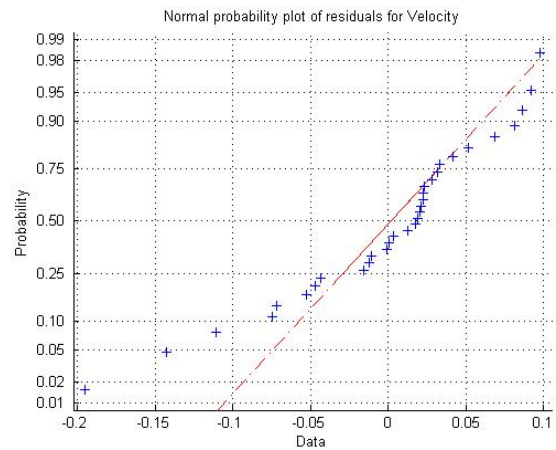


**Figure 8.48** Normal probability plot for the residuals.

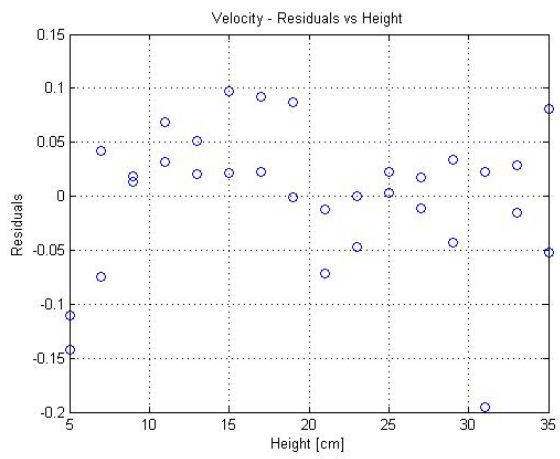


**Figure 8.49** Residuals plotted against height.

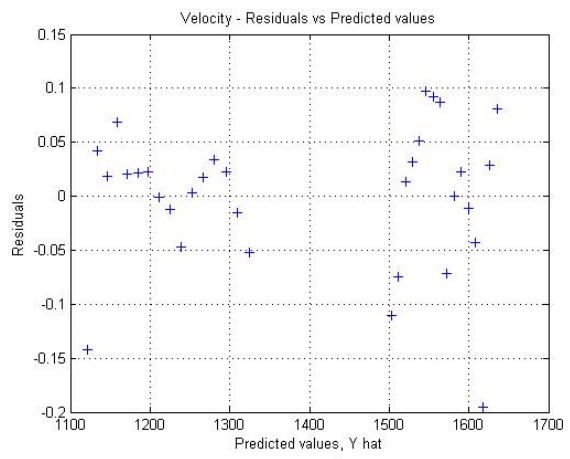


**Figure 8.50** Residuals plotted against predicted values.

## 9 Discussion/Analysis

### 9.1 Results

#### *Sinus waves*

When analyzing the difference in the energy containment, using the sinus waves, of the signals sent through the healthy contra the decayed tree, one can notice that the ratio between the energies suggests that the level of decay is enough to be noticeable. More of the signals energy passes through the healthy tree than that with decay. If more data from several samples and conditions would be collected maybe the variance in the results would reduce, resulting in a better outcome.

The difference in velocity did not give any significant difference at this stage of decay. It may be so that the degree of decay affects these results too profoundly.

#### *Chirp waves*

The analysis of frequency did show significant differences between healthy and decayed samples. When determining the energy ratio in some specific intervals of the coherence spectrum, it was concluded that a significantly larger amount of energy is contained by the healthy tree samples than the decayed, in these intervals. The intervals of interest where  $61 \leq I_1 \leq 98 \text{ kHz}$  and  $86 \leq I_2 \leq 112 \text{ kHz}$ . We can conclude that the signals contain these frequencies in larger density when passing through a healthy tree sample than through a decayed tree sample.

The analysis continued with the study of energy ratios between output and input signals. It was concluded that the energy ratio is significantly higher in healthy tree samples compared to decay. This means that the signals are significantly more dampened when passing through a decayed tree, than a healthy. There are several factors that could affect this result, but it can however give an impression of the difference in impact of signal. The result is consistent with the same analysis done with sinus waves.

The velocities were also analyzed and it was concluded that the signals passe significantly faster in healthy tree sample compared to the decayed.

### 9.2 Future work

Since using ultrasound is to determine decay, much of the analysis and probable methods of detection are based on the sound waves behavior in the tree. Since is no simple way to describe these behaviors, much due to the irregularities within each tree, it may be of interest to create a model e.g. using COMSOL.

As the chirp signal is sent into the tree the wave interacts with itself by reflection and interference within the tree before reaching the probe on the other side. By using a frequency sweep with fewer frequencies the received signal may be cleaner.

It would also be interesting to evaluate if the signal sent into the tree would improve in quality if an acoustic coupling medium is used.

Once a good signal was received the depth was recorded and used for all the other measurements. This was however conducted visually and might be improved using e.g.

pressure sensors instead. Incorrect placement of sensors can lead to incorrect results. When a possible future device would be used in the field the user would be able to avoid irregularities in the tree, such as knots, something that has not been taken under consideration in this thesis.

It would also be interesting to use a prototype on standing trees and evaluate what new obstacles occur when wanting to use the technique in the field. When using results from a standing tree the tree has not had a chance to dry out.

As mentioned earlier the measurements of the reflection were abandoned since the wave did not travel in a preferred way, but instead the shortest way between the exponential horns. If this problem would be solved the reflective measurements might be of greater interest since the measurements in the field can be conducted from the same side of the tree, thus easier.

### 9.3 Conclusions

The different approaches to the problem gave varying results. The contaminated wood was in the initial stages of decay, which makes it more difficult to see extreme differences in results when comparing the wood with decay to the healthy wood. However since it is in these initial stages of decay one is interested to be able to disforest, some of the results are encouraging.

The results from Series 1 showed that the difference in energy ratio between the output and input signals was not statically significant; however a difference could be noticed. The energy ratio for the decayed tree sample increased with height, approaching the values of the healthy tree sample.

The velocity analysis of the signals in Series 1 showed no significant difference between the healthy and decayed tree sample.

The analysis of data from Series 3 showed that there is a significant difference in the coherence contained in the frequencies analyzed. It could be concluded that the coherence was significantly higher in healthy compared to decayed in the frequencies  $61 \leq I_1 \leq 98 \text{ kHz}$ . This interval was decreased and the coherence was again proven to be significantly higher in healthy tree samples.

The energy ratio between the output and input signal indicates that more energy passes through the healthy compared to decayed tree samples.

The velocity analysis of data from series 3 showed that the signals pass faster in the healthy tree compared to the decayed tree samples.

With some more specimen and taking some of our suggestions for future work under consideration, a new, better way of detecting root and but rot in Norway Spruce as well as other species may be found. This study shows that there are some differences and significantly distinguished impacts on ultrasound signals passed through healthy, compared to decayed tree samples.

## 10 Appendix A

### 10.1 Tables from one frequency measurements – Series 1

#### 10.1.1 Energy analysis

<b>Healthy</b>			
<b>Height [cm]</b>	<b>Input energy</b>	<b>Output energy</b>	<b>Energy ratio</b>
2	1.7224	0.0105	0.0061
3	1.7266	0.0051	0.003
5	1.7115	0.0316	0.0185
7	1.7108	0.0063	0.0037
9	1.7128	0.12	0.007
11	1.714	0.0257	0.015
13	1.7029	0.0107	0.0063
15	1.7008	0.0188	0.011
17	1.7028	0.0057	0.0033
19	1.7071	0.0303	0.0177
21	1.6434	0.0013	0.000776
25	1.6489	0.0277	0.0168
27	1.6158	0.0453	0.028
29	1.636	0.0473	0.0289
31	1.6435	0.0048	0.0029
33	1.6496	0.0073	0.0044
35	1.7015	0.0199	0.0117
37	1.7175	0.0181	0.0105

**Table 10.1** *Energy ratios for healthy tree.*

<b>Decay</b>			
<b>Height [cm]</b>	<b>Input energy</b>	<b>Output energy</b>	<b>Energy ratio</b>
2	1.6727	0.0028	0.0017
4	1.6728	0.003	0.0018
6	1.674	0.0014	0.000831
8	1.6722	0.0029	0.0017
10	1.6702	0.0027	0.0016
12	1.6728	0.003	0.0018
14	1.6589	0.0014	0.000829
16	1.6691	0.0028	0.0017
18	1.6659	0.0064	0.0039
21	1.6689	0.0036	0.0022
23	1.664	0.0028	0.0017
25	1.6666	0.0027	0.0016
27	1.6581	0.002	0.0012
29	1.6604	0.0138	0.0083
31	1.6232	0.0123	0.0076
33	1.6674	0.0119	0.0071
35	1.6685	0.0249	0.0149
37	1.6689	0.02	0.012

**Table 10.2** *Energy ratios for decayed tree.*

### 10.1.2 Velocity analysis

<b>Healthy</b>			
<b>Height [cm]</b>	<b>Passing time [micro sek]</b>	<b>Diameter of the tree [cm]</b>	<b>Velocity [m/s]</b>
2	155	21.3	1374.194
3	143	21.3	1489.51
5	170	21.3	1252.941
7	150	21.3	1420.00
9	148	21.3	1439.189
11	148	21.3	1439.189
13	151	21.3	1410.596
15	144	21.3	1479.167
17	145	21.3	1468.966
19	145	21.3	1468.966
21	152	21.3	1401.316
23	178	21.3	1196.629
25	171	21.3	1245.614
27	153	21.3	1392.157
28	145	21.3	1468.966
29	153	21.3	1392.157
31	148	21.3	1439.189
33	148	21.3	1439.189
35	144	21.3	1479.167
37	143	21.3	1489.51

**Table 10.3** *The velocity measurements from the healthy tree, with one frequency input.*

<b>Decay</b>			
<b>Height [cm]</b>	<b>Passing time [micro sek]</b>	<b>Diameter of the tree [cm]</b>	<b>Velocity [m/s]</b>
2	190	22.9	1205.263
4	142	22.9	1612.676
6	160	22.9	1431.25
8	184	22.9	1244.565
10	198	22.9	1156.566
12	179	22.9	1279.33
14	192	22.9	1192.708
16	186	22.9	1231.183
18	186	22.9	1231.183
21	180	22.9	1272.222
22	181	22.9	1265.193
23	181	22.9	1265.193
25	180	22.9	1272.222
27	151	22.9	1516.556
29	152	22.9	1506.579
31	146	22.9	1568.493
33	134	22.9	1708.955
35	117	22.9	1957.265
37	140	22.9	1635.714
39	107	22.9	2140.187

**Table 10.4** *The velocity measurements from the decayed tree, with one frequency input.*

## 10.2 Tables from chirp measurements analysis – Series 3

### 10.2.1 Frequency analysis

The tables used in section 7.2 *Frequency Analysis* are found below. Tables 10.5-10.6 show the ratios from measurement where the coherence function is divided in two intervals. And tables A3-A4 are from measurements with three intervals.

Healthy Tree Stock height (cm)	Thompson, ratio in $I_1$	Peak Matched Method, ratio in $I_1$
5	0.736	0.7714
7	0.8064	0.8503
9	0.7868	0.7764
11	0.5194	0.5239
13	0.709	0.6766
15	0.7321	0.6822
17	0.5938	0.6073
19	0.7383	0.7623
21	0.522	0.5511
23	0.6793	0.6616
25	0.6855	0.696
27	0.6868	0.7013
29	0.699	0.7128
31	0.7569	0.7569
33	0.7497	0.7542
35	0.7313	0.7511

**Table 10.5** The coherence ratio for the coherence spectrum contained in  $I_1$  for the healthy tree stock.

Decayed Tree Stock height (cm)	Thompson, ratio in $I_1$	Peak Matched Method, ratio in $I_1$
5	0.3547	0.2434
7	0.2851	0.2254
9	0.2508	0.2122
11	0.3611	0.355
13	0.5901	0.4965
15	0.6652	0.5731
17	0.4801	0.336
19	0.2718	0.2357
21	0.4422	0.3508
23	0.3093	0.2362
25	0.3822	0.3161
27	0.4297	0.3684
29	0.5397	0.4998
31	0.5059	0.4206
33	0.4819	0.4508
35	0.5303	0.4514

**Table 10.6** The coherence ratio for the coherence spectrum contained in  $I_1$  for the decayed tree stock.

### 10.2.2 Coherence ratio in interval $I_2$ of coherence spectrum (Section 8.3.2)

	Healthy	Decay
Height [cm]	Coherence ratio in $I_2$	Coherence ratio in $I_2$
5	0.3577	0.3982
7	0.3035	0.2695
9	0.4484	0.3022
11	0.4801	0.3499
13	0.5265	0.3405
15	0.5689	0.3412
17	0.3187	0.3268
19	0.4267	0.4286
21	0.524	0.3338
23	0.5029	0.3256
25	0.4783	0.4076
27	0.4391	0.2326
29	0.4422	0.3557
31	0.5057	0.2674
33	0.406	0.4862
35	0.3886	0.2956

**Table 10.7** Coherence ratio.

### 10.2.3 Energy analysis

Healthy			
Height [cm]	Energy In	Energy Out	Energy Ratio
5	2441.1	122.1538	0.050040474
7	2477.8	151.3224	0.061071273
9	2473.2	134.0286	0.054192382
11	2496	49.3505	0.019771835
13	2504.9	74.2265	0.02963252
15	2482.4	86.886	0.035000806
17	2418.8	79.4102	0.032830412
19	2495.6	256.9944	0.102979003
21	2441	23.8046	0.009751987
23	2461.1	33.451	0.01359189
25	2449.9	61.4999	0.025103025
27	2437.8	88.7158	0.036391747
29	2460.7	106.0339	0.04309095
31	2450.8	512.9919	0.209316101
33	2424.2	1244.4	0.513323983
35	2440.9	1007.5	0.412757589

**Table 10.8** Energies from signals through healthy tree sample.

Decay			
Height [cm]	Energy In	Energy Out	Energy Ratio
5	389.7317	0.8855	0.002272076
7	385.5734	1.2821	0.003325178
9	364.8456	1.1163	0.00305965
11	375.0722	0.8809	0.002348614
13	383.0282	1.3945	0.003640724
15	369.017	1.4327	0.003882477
17	387.0004	1.7336	0.004479582
19	385.7314	1.533	0.003974268
21	382.7421	1.6365	0.004275725
23	375.2602	1.2453	0.003318497
25	370.856	1.5988	0.004311107
27	377.5342	1.7536	0.004644877
29	375.7331	1.6494	0.004389818
31	384.7397	1.8604	0.004835477
33	364.0225	2.3423	0.006434492
35	375.9882	2.482	0.006601271

**Table 10.9** Energies from signals through decayed tree sample.

#### 10.2.4 Velocity analysis

Healthy			
Height [cm]	Passing time [ $\mu$ s]	Diameter [mm]	Velocity [m/s]
5	235.6	229	971.9864
7	193.8	229	1181.631
9	196.1	229	1167.772
11	184.5	229	1241.192
13	191.5	229	1195.822
15	189.2	229	1210.359
17	186.8	229	1225.91
19	189.2	229	1210.359
21	189.2	229	1210.359
23	193.8	229	1181.631
25	182.2	229	1256.861
27	177.6	229	1289.414
29	172.9	229	1324.465
31	172.9	229	1324.465
33	177.6	229	1289.414
35	182.2	229	1256.861

**Table 10.10** Velocity for signals through healthy tree sample.

Decay			
Height [cm]	Passing time [ $\mu$ s]	Diameter [mm]	Velocity [m/s]
5	159.7	215	1346.274
7	153.2	215	1403.394
9	139.6	215	1540.115
11	136.2	215	1578.561
13	132.8	215	1618.976
15	126.1	215	1704.996

17	126.1	215	1704.996
19	126.1	215	1704.996
21	146.9	215	1463.581
23	135.9	215	1582.046
25	132.2	215	1626.324
27	135.9	215	1582.046
29	139.6	215	1540.115
31	161.6	215	1330.446
33	128.5	215	1673.152
35	121.2	215	1773.927

**Table 10.11** *Velocity for signals through decayed tree sample.*

## 11 Bibliography

Bucur, V. (2006), *Acoustics of Wood*, Berlin Heidelberg New York: Springer Verlag

G. Lindgren, H. Rootzén, M. Sandsten, *Stationary Stochastic Processes*, Lund University, 2009

M. Hansson, G. Salomonsson, *A Multiple Window Method for Estimation of Peak Spectra*, 1997

Rawlings, J.O., Pantula, S.G., Dickey, D.A.: *Applied Regression Analysis - A Research Tool*, 2ed, Springer

<http://www-gran.slu.se/Webbok/PDFdokument/Biologi.pdf>

<http://www.fs.fed.us/database/feis/plants/tree/picabi/all.html>

[http://www.skogforsk.se/sv/KunskapDirekt/Gallra/Rota-och-andra-svampskador-/](http://www.skogforsk.se/sv/KunskapDirekt/Gallra/Rota-och-andra-svampskador/)

The Swedish Forest Industries. (2010), *Facts and Figures 2010*, Brommatryck & Brolins  
[www.gran.slu.se/Webbok/PDFdokument/Rötbok%20fullständig%201%2020060626.pdf](http://www.gran.slu.se/Webbok/PDFdokument/Rötbok%20fullständig%201%2020060626.pdf)

[http://www.websitefolder.net/rotfinder/Historien\\_om\\_Rotfinder.asp](http://www.websitefolder.net/rotfinder/Historien_om_Rotfinder.asp)

X. Wang, F. Divos, C. Pilon, B. Brashaw, R. Ross & R. Pellerin (2004), *Assessment of Decay in Standing Timber Using Stress Wave Timing Nondestructive Evaluation Tools*, U.S. Department of Agriculture, Forest Service, Forest Products Laboratory, Madison, WI.

<http://www.skogssverige.se/index.cfm>